Original Article

Development of a novel angiogenesis-related lncRNA signature to predict the prognosis and immunotherapy of glioblastoma multiforme

Binbin Zhang[1], Yaling Cheng[1], Ruichun Li[1], Minxue Lian[1], Shiwen Guo[1], Chen Liang[1,2]

[1]Department of Neurosurgery, First Affiliated Hospital of Xi'an Jiaotong University, Xi'an, China; [2]Department of Radiology Medical Physics, University Medical Center Freiburg, Faculty of Medicine, University of Freiburg, Freiburg, Germany

Contributions: (I) Conception and design: C Liang (II) Administrative support: S Guo; (III) Provision of study materials or patients: R Li, M Lian; (IV) Collection and assembly of data: B Zhang, Y Cheng; (V) Data analysis and interpretation: B Zhang, Y Cheng; (VI) Manuscript writing: all authors; (VII) Final approval of manuscript: all authors.

Correspondence to: Dr. Chen Liang. Department of Neurosurgery, First Affiliated Hospital of Xi'an Jiaotong University, Xi'an 710061, China. Email: liangchen01@xjtu.edu.cn.

Background: Long noncoding RNA (lncRNA) can regulate tumorigenesis, angiogenesis, proliferation, and other tumor biological behaviors, and is closely related to the growth and progression of glioma. The purpose of this research was to investigate the role of angiogenesis-related lncRNA in the prognosis and immunotherapy of glioblastoma multiforme (GBM).

Methods: Differential analysis was carried out to acquire angiogenesis-related differentially expressed lncRNAs (AR-DElncRNAs). The AR-DElncRNAs were then subjected to univariate Cox and least absolute shrinkage and selection operator (LASSO) analyses to construct a prognostic model. Based on the median risk score, patients were classified into high-risk and low-risk groups. Kaplan-Meier survival analysis was conducted to estimate the prognostic value of the prognostic model. In addition, a nomogram was built to predict individual survival probabilities by combining clinicopathological characteristics and a prognostic model. Furthermore, immune infiltration, immunotherapy, and drug sensitivity analyses were administered to investigate the differences between the high- and low-risk groups.

Results: We identified 3 lncRNAs (DGCR5, PRKAG2-AS1, and ACAP2-IT1) that were significantly associated with the survival of GBM patients from the 255 AR-DElncRNAs based on univariate Cox and LASSO analyses. Then, a prognostic model was structured according to these 3 lncRNAs, from which we found that high-risk GBM patients had a worse prognosis than that of low-risk patients. Moreover, the risk score was determined to be an independent prognostic factor [hazard ratio (HR) =1.444; 95% confidence interval (CI): 1.014–2.057; P<0.05]. The immune microenvironment analysis revealed that the immune score, stromal score, and Estimation of STromal and Immune cells in MAlignant Tumor tissues using Expression data (ESTIMATE) score were significantly higher in the high-risk group than in the low-risk group. Neutrophils, macrophages, immature dendritic cells (iDCs), natural killer (NK) CD56dim cells, activated DCs (aDCs), and uncharacterized cells were different in the high- and low-risk groups. In addition, the high-risk group had a stronger sensitivity to immunotherapy. Furthermore, the sensitivity of 28 potential chemotherapeutic drugs differed significantly between the high- and low-risk groups.

Conclusions: A novel angiogenesis-related lncRNA signature could be used to predict the prognosis and treatment of GBM.

Keywords: Glioblastoma multiforme (GBM); angiogenesis; long noncoding RNA (lncRNA); prognosis; immunotherapy

Submitted Jun 07, 2022. Accepted for publication Oct 17, 2022. Published online Dec 22, 2022.
doi: 10.21037/tcr-22-1592
View this article at: https://dx.doi.org/10.21037/tcr-22-1592

Introduction

Glioma is one of the most common human primary brain tumors and has a poor prognosis (1,2). Among all gliomas, glioblastoma multiforme (GBM) is the most frequent, accounting for 55% of gliomas globally (3). Despite the standard treatment of surgery combined with radiotherapy and chemotherapy, the prognosis of patients with GBM is still unsatisfactory (2). Therefore, it is urgent to find more effective treatments for glioblastoma. Prognostic analysis can provide new ideas for treatment. However, due to the complicated heterogeneity of glioblastoma, the prognosis often varies across different patients (4). Angiogenesis levels of glioma are closely related to tumor malignancy and prognosis (5). Angiogenesis is a complex multistep biological process that can provide nutrition and oxygen to the glioblastoma, which promotes solid tumor growth and progression (6). An animal study has confirmed that inhibiting angiogenesis in a GBM animal model can inhibit tumor growth (7). Furthermore, a clinical study has also shown that angiogenesis inhibitors can improve the prognosis of patients with GBM (8). Therefore, antiangiogenic therapy has been considered a very promising treatment strategy for GBM.

Long noncoding RNAs (lncRNAs) are transcripts longer than 200 nucleotides that do not encode proteins (9). The abnormal expression of functional lncRNAs regulates the tumorigenesis (10), proliferation (11), development (12), and other biological behaviors of glioma. A previous study has shown a close relationship between lncRNAs and angiogenesis in glioma (13). Therefore, the study of angiogenesis-related lncRNAs can provide a theoretical basis for revealing the angiogenic mechanism of GBM.

Our study aimed to investigate the role of angiogenesis-related lncRNAs in the prognosis and immunotherapy of GBM and construct a prognostic model according to lncRNAs to predict the prognosis and treatment of GBM. We identified differentially expressed lncRNAs (DE-lncRNAs) in GBM patients and established an angiogenesis-related prognostic signature using The Cancer Genome Atlas (TCGA)-GBM cohort. Then, we estimated the prognostic value of this prognostic model. Meanwhile, a nomogram was built to predict individual survival probabilities by combining clinicopathological characteristics and a prognostic model. Furthermore, immune infiltration, immunotherapy, and drug sensitivity analyses were administered to further confirm the predictive and prognostic value of the prognostic model. We present the following article in accordance with the TRIPOD reporting checklist (available at https://tcr.amegroups.com/article/view/10.21037/tcr-22-1592/rc).

Methods

Data collection

Transcriptome sequencing (3 levels) data and corresponding clinical information of the TCGA-GBM cohort, including 158 GBM samples with fully available survival data, 11 GBM samples with unavailable survival data, and 5 normal tissue samples, were obtained from TCGA database (https://tcga-data.nci.nih.gov/tcga/) (Table S1). Moreover, transcriptome sequencing data of 133 GBM samples with fully available survival data in the mRNAseq-693 dataset were downloaded and used as a validation cohort from the Chinese Glioma Genome Atlas (CGGA) database (http://www.cgga.org.cn/) (Table S2). Additionally, a total of 48 angiogenesis-related genes were acquired from the gene set enrichment analysis (GSEA)-Molecular Signatures Database v7.4 (http://www.gseamsigdb. org/gsea/msigdb/index.jsp).

Screening of angiogenesis-related differentially expressed lncRNAs (AR-DElncRNAs)

Using the "limma" package (version 3.44.3) in R (The R Foundation for Statistical Computing, Vienna, Austria), the DE-lncRNAs were identified between 5 normal and 169 tumor tissues in the TCGA-GBM cohort based on adjusted standards of $P<0.05$ and $|\log2 \text{ (fold change)}| >1$. The "ggplot" package (version 3.3.3) was used to plot the volcano plot. The Spearman test was then used to perform a correlation analysis between 48 angiogenesis-related genes and lncRNAs of the GBM expression matrix to screen angiogenesis-related lncRNAs. The screening criteria were $|cor| >0.3$ and $P<0.01$. Then, the angiogenesis-related lncRNAs were intersected with the DE-lncRNAs as AR-DElncRNAs.

Construction and validation of an angiogenesis-related lncRNA signature

First, GBM samples in the TCGA-GBM cohort were randomly divided into a training set (n=111) and an internal validation set (n=47) at a ratio of 7:3. The clinicopathologic characteristic of patients with GBM in the training set, validation set, and CGGA_693 cohort are shown in *Table 1*.

Table 1 Clinicopathologic characteristics of GBM patients in TCGA and CGGA cohorts

Characteristic	TCGA-GBM			CGGA_693 (n=133)
	Total (n=158)	Training set (n=111)	Testing set (n=47)	
Age (years), mean (± SD)	59.6 (±13.8)	59.0 (±12.9)	61.0 (±15.7)	52.3 (±13.2)
Gender, n (%)				
Female	52 (32.9)	36 (32.4)	16 (34.0)	53 (39.8)
Male	95 (60.1)	65 (58.6)	30 (63.8)	80 (60.2)
Unclear	11 (7.0)	10 (9.0)	1 (2.1)	–
Vital, n (%)				
Alive	29 (18.4)	19 (17.1)	10 (21.3)	23 (17.3)
Dead	128 (81.0)	91 (82.0)	37 (78.7)	110 (82.7)
Unclear	1 (0.6)	1 (0.9)	–	–
KPS, mean (± SD)	75.2 (±14.2)	75.8 (±14.2)	74.2 (±14.4)	–
Radio_status				
Treated	129 (81.6)	94 (84.7)	35 (74.5)	110 (82.7)
Untreated	20 (12.7)	11 (9.9)	9 (19.1)	19 (14.3)
Unclear	9 (5.7)	6 (5.4)	3 (6.4)	4 (3.0)
Chemo_status, n (%)				
Treated	127 (80.4)	91 (82.0)	36 (76.6)	109 (82.0)
Untreated	21 (13.3)	12 (10.8)	9 (19.1)	19 (14.3)
Unclear	10 (6.3)	8 (7.2)	2 (4.3)	5 (3.7)
Original subtype, n (%)				
Classical	37 (23.4)	24 (21.6)	13 (27.7)	–
G-CIMP	8 (5.1)	6 (5.4)	2 (4.3)	–
Mesenchymal	45 (28.5)	29 (26.1)	16 (34.0)	–
Neural	26 (16.4)	21 (18.9)	5 (10.6)	–
Proneural	29 (18.4)	20 (18.0)	9 (19.1)	–
Unclear	13 (8.2)	11 (9.9)	2 (4.3)	–
IDH status, n (%)				
Mutant	10 (6.3)	8 (7.2)	2 (4.2)	21 (15.8)
WT	132 (83.5)	90 (81.1)	42 (89.4)	105 (78.9)
Unclear	16 (10.1)	13 (11.7)	3 (6.4)	7 (5.3)
MGMT promoter status, n (%)				
Methylated	51 (32.3)	34 (30.6)	17 (36.2)	63 (47.4)
Unmethylated	67 (42.4)	44 (39.6)	23 (48.9)	54 (40.6)
Unclear	40 (25.3)	33 (29.7)	7 (14.9)	16 (12.0)
1p19q_status, n (%)				
Codel	–	–	–	4 (3.0)
Noncodel	–	–	–	104 (78.2)
Unclear	–	–	–	25 (18.8)

CGGA, Chinese Glioma Genome Atlas; Codel, codeletion; GBM, glioblastoma multiforme; G-CIMP, Glioma CpG island methylator phenotype; IDH, isocitrate dehydrogenase; KPS, Karnofsky Performance Scale; MGMT, O6-methylguanine-DNA methyltransferase; SD, standard deviation; TCGA, The Cancer Genome Atlas; WT, wild type.

Following this, a univariate Cox regression analysis was exploited to select overall survival (OS)-associated lncRNAs in the training set (P<0.05). To further narrow down the candidate lncRNAs, we applied the least absolute shrinkage and selection operator (LASSO) algorithm to prevent model overfitting by using the "glmnet" package (version 4.1-1) in R.

A risk score was calculated by LASSO regression coefficients using the following formula:

$$\text{Riskscore} = \sum_{i=1}^{n} \text{coef}\left(gene_i\right) * \exp r\left(gene_i\right) \quad [1]$$

where coef ($gene_i$) is the risk coefficient, and expr ($gene_i$) is the expression level of prognostic lncRNAs. Based on the median risk score, samples in the training set were divided into high- and low-risk groups. Kaplan-Meier survival analysis was used to determine the survival difference between these 2 risk groups. To assess the performance of the prognostic model, area under the receiver operating characteristic (ROC) curve (AUC) analysis was conducted using the "timeROC" package (version 1.0.3) in R. In addition, the risk scores of patients with GBM in both the internal validation set and external validation set were calculated using the same formula as the methods mentioned above and used to validate the performance of the risk signature separately.

Correlation analysis of the risk model and clinical characteristics

To further explore the correlation between the risk signature and clinical characteristics, we compared the risk scores among patients with GBM with different clinical characteristics in the TCGA-GBM cohort, including age (≥65 *vs.* <65), sex (female *vs.* male), O6-methylguanine-DNA methyltransferase (MGMT) status, and isocitrate dehydrogenase 1 (IDH1), and subtype. The results were visualized by drawing violin plots with the "ggpubr" package (version 0.4.0).

Independent prognostic factor analysis and nomogram construction

Univariate and multivariate Cox regression analyses were performed to investigate the prognostic significance of clinical characteristics and risk scores in the TCGA-GBM cohort. The risk score and clinicopathological factors, including age, sex, MGMT status, IDH1 status, and pathological subtypes, were used to perform univariate Cox analysis to screen prognostic factors. Moreover, prognostic factors (P<0.05) were uploaded to multivariate Cox analysis to identify independent prognostic factors. Based on the results of the multivariate analysis, we applied the "rms" package (version 6.2-0) in R to create a nomogram for guiding clinical decision-making. The calibration curve was used to assess the predictive accuracy of the nomogram.

Construction of a competing endogenous RNA (ceRNA) regulatory network of the prognostic lncRNA signature

To predict the ceRNA network of the lncRNA signature, we used the StarBase 2.0 database (https://starbase.sysu.edu.cn/starbase2/) to predict lncRNA-microRNA (miRNA) targeting relationships with a screening condition of stringency (≥1) and used the miRWalk database (http://mirwalk.umm.uni-heidelberg.de/) to predict the miRNA-messenger RNA (mRNA) relationship pairs with a screening threshold of 1. The predicted target genes were intersected with the downregulated mRNAs according to the regulatory relationship of ceRNA (the lncRNA and mRNA expression trends were the same), and genes with Pearson correlation of $|cor| > 0.5$ and P<0.05 were used to construct the ceRNA network. Finally, the targeting relationships between lncRNAs, miRNAs, and mRNAs were imported into Cytoscape (version 3.8.2) to construct the lncRNA-miRNA-mRNA network.

Functional enrichment analysis

To further examine the prognostic features of the functions performed by lncRNA target genes, this study used the "clusterProfiler" package (version 3.18.0) to perform an enrichment analysis based on the Gene Ontology (GO) and Kyoto Encyclopedia of Genes and Genomes (KEGG) databases. Doing so enabled us to identify the common functions and related pathways of a large number of genes within the key gene set. The GO system consists of 3 parts: biological process, molecular functions, and cellular components. GO terms and KEGG pathways were selected if the P value was less than 0.05 and the count showed 2 or more.

Assessment of tumor immune cell infiltration

To explore immunological differences between the high- and low-risk groups, we performed Estimation of STromal and Immune cells in MAlignant Tumor tissues using Expression

data (ESTIMATE) analysis using the "estimate" package (version 1.0.13) to obtain the tumor tissue immune score, stromal score, and ESTIMATE score of both combined. Single-sample gene set enrichment analysis (ssGSEA) was employed to analyze the differences in immune infiltration between the high- and low-risk groups. The abundance of the 24 immune cells was visualized using "ggplot2" (version 3.3.3) and "ggpubr" (version 0.4.0) to draw box line plots. In addition, the proportion of 22 immune cell species in TCGA-GBM was calculated using the CIBERSORT algorithm (version 1.03) and the LM22 gene set. The results of scoring 22 immune cell species were visualized by drawing violin plots using the "vioplot" package (version 0.3.7). In addition, we also used the EPIC, MCP-Counter, and quanTIseq methods in the "immunedeconv" package to obtain the percentage of different immune cells. The proportion of immune and nonimmune cells in the tumor microenvironment was analyzed using the online database xCell (https://xcell.ucsf.edu/). Finally, leukocyte fraction data for the GBM samples were obtained from the Genomic Data Commons (GDC; https://gdc.cancer.gov/about-data/publications/panimmune) database, and then differences between high- and low-risk groups were compared using a rank sum test.

Immunotherapy analysis

First, we compared the expression of immune checkpoint genes in the high- and low-risk groups. Then, differences in immunotherapy sensitivity between the high- and low-risk groups were assessed using Tumor Immune Dysfunction and Exclusion (TIDE). Using the submap method, we compared differences in sensitivity of GBM to different immunotherapies. According to different therapeutic targets and responses, the sensitivity was divided into programmed cell death protein 1 (PD-1)-response (R), PD-1-no response (noR), cytotoxic T-lymphocyte protein 4 (CTLA4)-R, and CTLA4-noR.

Drug susceptibility analysis

To further examine whether risk scores could be used to predict the effectiveness of chemotherapy this study used the "pRRophetic" package (version 0.5) to calculate the half maximal inhibitory concentration (IC50) of the GBM sample for drugs in the Genomics of Drug Sensitivity in Cancer (GDSC) database (https://www.cancerrxgene.org/). The differences in IC50 of chemotherapeutic agents between the high- and low-risk groups were compared according to the calculated results.

Statistical analysis

R language was the main tool used to generate figures and perform the statistical analysis. The use of several R language packages is described above. A P value less than 0.05 was considered to indicate a statistically significant difference.

Ethical statement

The study was conducted in accordance with the Declaration of Helsinki (as revised in 2013).

Results

Identification of prognostic angiogenesis-related lncRNAs in GBM

A total of 277 lncRNAs with significant expression differences in TCGA-GBM were enrolled in this study, of which 104 were upregulated and 173 were downregulated (*Figure 1A*). Spearman correlation analysis revealed a total of 5,681 lncRNAs associated with 48 angiogenic genes in the lncRNA expression matrix of GBM. Candidate lncRNAs were intersected with DE-lncRNAs to obtain 255 AR-DElncRNAs (*Figure 1B*). Univariate Cox regression analysis then identified 3 AR-DElncRNAs that were significantly associated with OS (P<0.05) (*Figure 1C*). The 3 most important prognosis-related lncRNAs (DGCR5, PRKAG2-AS1, and ACAP2-IT1) were further screened out using LASSO analysis (*Figures 1D,1E*).

Establishment and validation of the angiogenesis-related lncRNA signature

A risk model was constructed using the expression of the 3 identified prognosis-related AR-DElncRNAs and their corresponding regression coefficients in the TCGA-GBM training set. The risk score was calculated as follows: risk score =0.31 × DGCR5 + 0.07× PRKAG2-AS1 + 0.02 × ACAP2-IT1. All patients were divided into high- and low-risk groups based on the median risk score of 0.9195 in the TCGA-GBM training set. *Figure 2A* shows the distribution of survival status and risk score and indicates that more deaths occurred in the high-risk group. *Figure 2B*

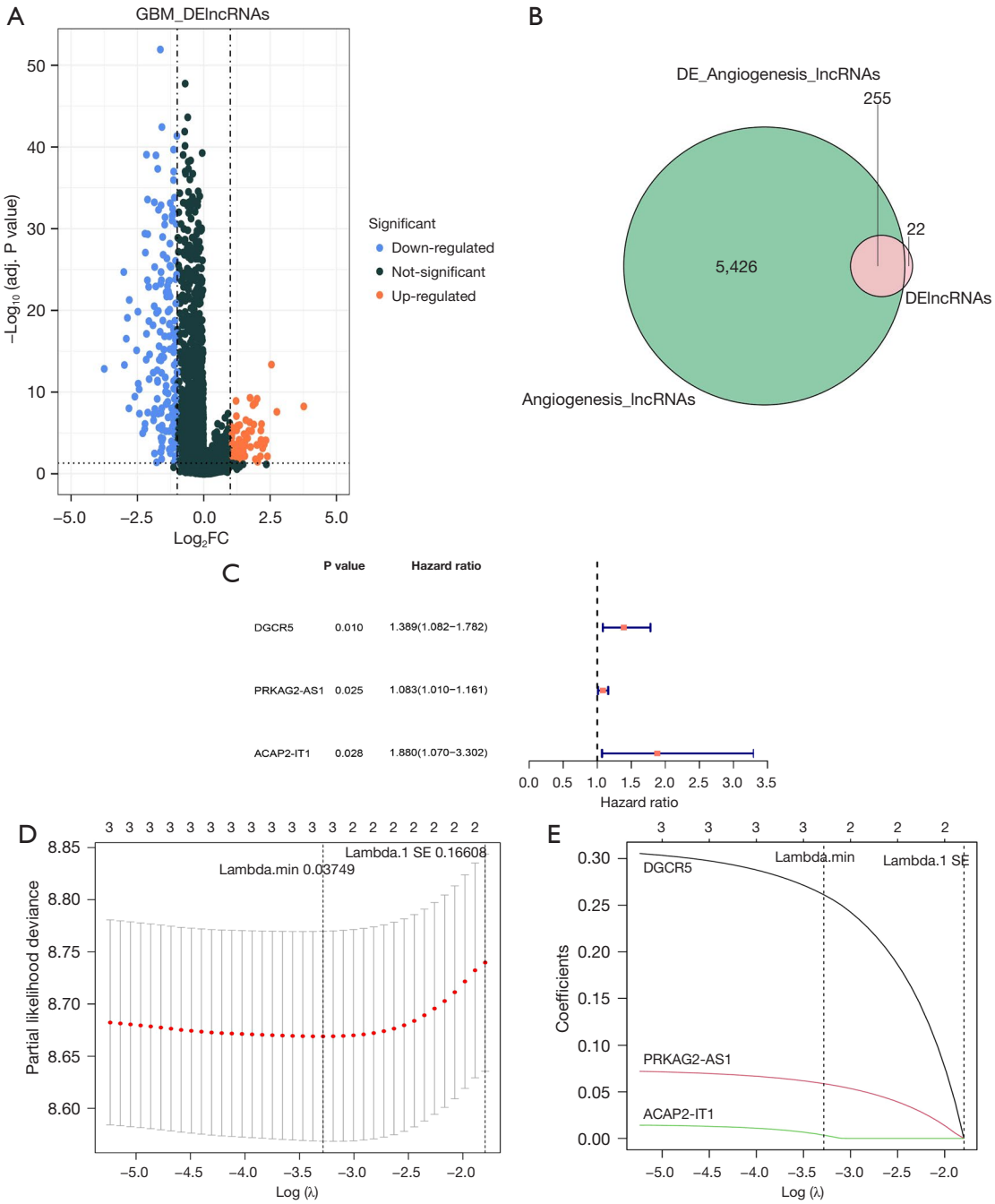

Figure 1 Identification of prognostic angiogenesis-related lncRNAs in GBM. (A) DE-lncRNAs in TCGA-GBM. (B) The selection of differentially expressed AR-DElncRNAs. (C) Three AR-DElncRNAs significantly associated with the OS of GBM patients were selected. (D,E) LASSO variable screening process. AR-DElncRNAs, angiogenesis-related differentially expressed lncRNAs; DE-lncRNAs, differentially expressed lncRNAs; lncRNAs, long noncoding RNAs; LASSO, least absolute shrinkage and selection operator; FC, fold change; GBM, glioblastoma multiforme; TCGA, The Cancer Genome Atlas; OS, overall survival; min, minimum; SE, standard error.

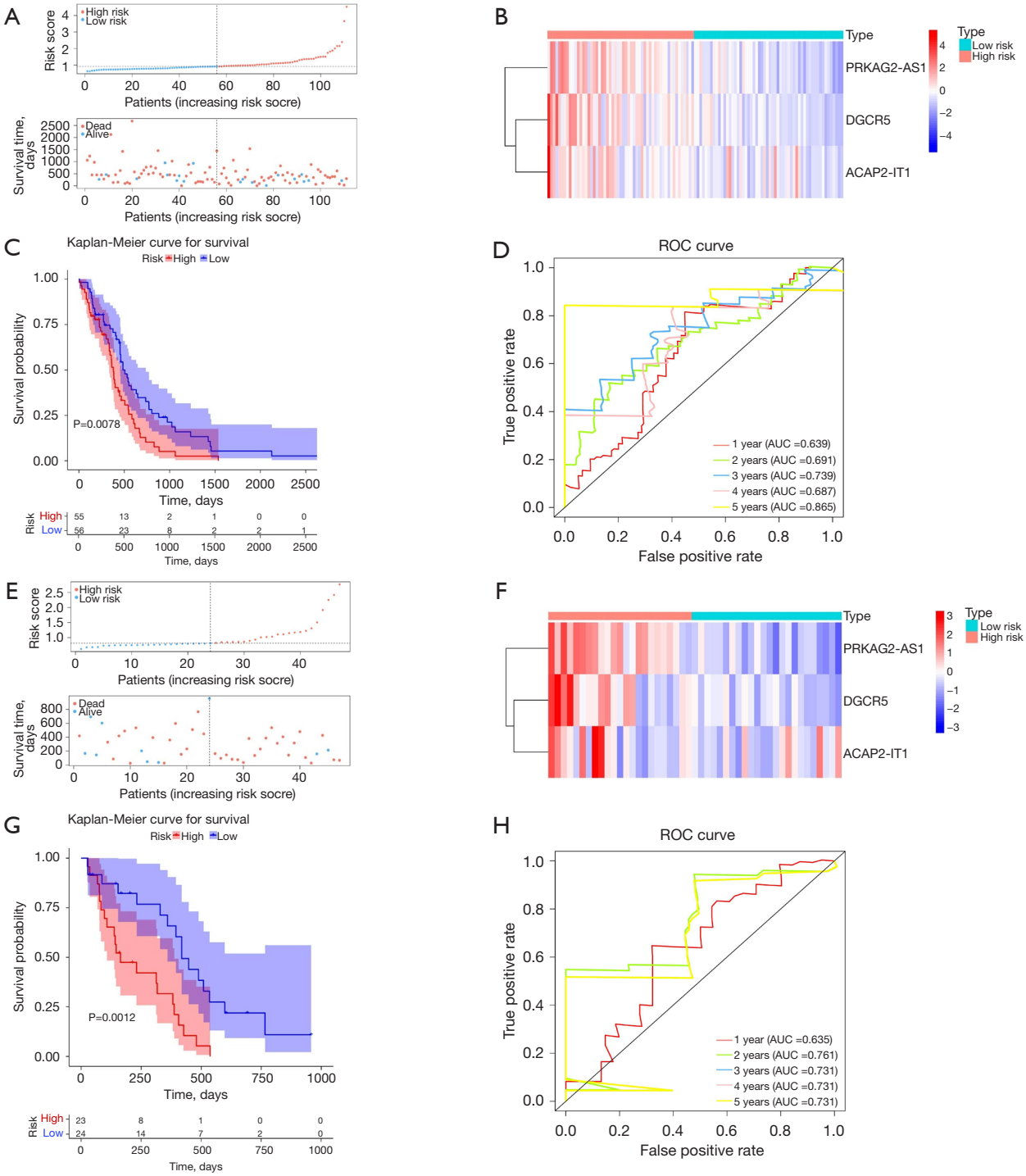

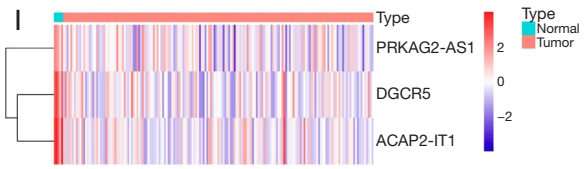

Figure 2 Validation of the angiogenesis-related lncRNA signature. (A) The distribution of survival status and risk score of patients with GBM in TCGA-GBM training set. (B) The expression characteristics of the 3 identified prognosis-related differentially expressed AR-DElncRNAs in the training set. (C) Survival analysis between the 2 risk subgroups in the training set. (D) ROC curve for patient survival of the training set. (E,F) The distribution of the survival status and risk score of patients with GBM and the expression characteristics of the 3 identified prognosis-related AR-DElncRNAs in the internal validation set. (G) Survival analysis between the 2 risk subgroups in the internal validation set. (H) ROC curve for patient survival of the internal validation set. (I) The unsupervised heatmap of the expression of 3 prognosis-related AR-DElncRNAs. AR-DElncRNAs, angiogenesis-related differentially expressed lncRNAs; AUC, area under the curve; GBM, glioblastoma multiforme; lncRNAs, long noncoding RNAs; ROC, receiver operating characteristic; TCGA, The Cancer Genome Atlas.

displays the expression characteristics of these 3 identified prognostic signatures. High expression of the 3 prognostic signatures occurred in patients with high-risk scores. To verify the survival differences between the 2 groups, we performed survival analysis on all cases and found that the OS of patients in the high-risk group was significantly worse than that in the low-risk group (*Figure 2C*; P<0.05). ROC curves were plotted for patient survival from 1 to 5 years, and all AUC values were above 0.6, indicating good efficacy of the risk model (*Figure 2D*).

Validation sets showed better prediction accuracy of our 3 prognostic signatures. In the internal validation set TCGA-GBM, patients were classified into high- and low-risk groups according to a median risk score of 0.8113. Patients in the high-risk group were found to have a worse prognosis and higher expression of the 3 prognostic signatures than those in the low-risk group (*Figures 2E-2G*). The AUC values of the patients' ROC curve analysis from 1 to 5 years were all over 0.6 (*Figure 2H*). Consistent results were obtained in the external validation set mRNAseq-693 (Figure S1). We plotted the unsupervised heatmap of the expression of the 3 lncRNAs (*Figure 2I*).

Differences in risk scores for clinical characteristics

To further investigate the prognosis of clinicopathological characteristics, the Pearson correlation between clinicopathological factors and risk score was analyzed. The correlations between the risk score and sex, age, MGMT status, and IDH1 status were not significant (P>0.05; *Figures 3A-3D*). Among the subtypes, the proneural subtypes had a significantly lower risk score than did the mesenchymal subtypes (P<0.05; *Figure 3E*).

The lncRNA signature as an independent prognostic factor and construction of the nomogram

To estimate critical prognostic factors and the clinical suitability of the prognostic model, we carried out univariate and multivariate Cox analyses, from which we identified independent prognostic factors and formulated a nomogram. The results of the univariate analysis showed that risk score, age, MGMT status, and IDH1 status were statistically significant (P<0.05; *Figure 4A*). After the multivariate Cox analysis, we found that the risk score was a dependable independent prognostic factor for patients with GBM [hazard ratio (HR) =1.444; P=0.042; *Figure 4B*]. A predictive nomogram was constructed to predict the 1-, 2-, and 3-year survival rates of GBM cases based on the risk score, age, and MGMT status (*Figure 4C*). The concordance index of the nomogram was calculated to be 0.6742836, indicating that the model was effective in predicting 1 to 3-year survival (*Figures 4D-4F*).

Construction of the ceRNA network of the lncRNA signature and functional analysis

To better investigate the regulatory mechanism of the lncRNA signature in GBM, we constructed a lncRNA signature-related ceRNA network. First, 29 miRNAs with targeting relationships with lncRNAs were obtained using the Starbase2.0 database (lncRNA-miRNA). Then, the target mRNAs of 29 miRNAs were predicted in the miRWalk database. According to the expression downregulation characteristics of the lncRNA signatures ACAP2-IT1, PRKAG2-AS1, and DGCR5, the predicted target genes were intersected with the differentially downregulated

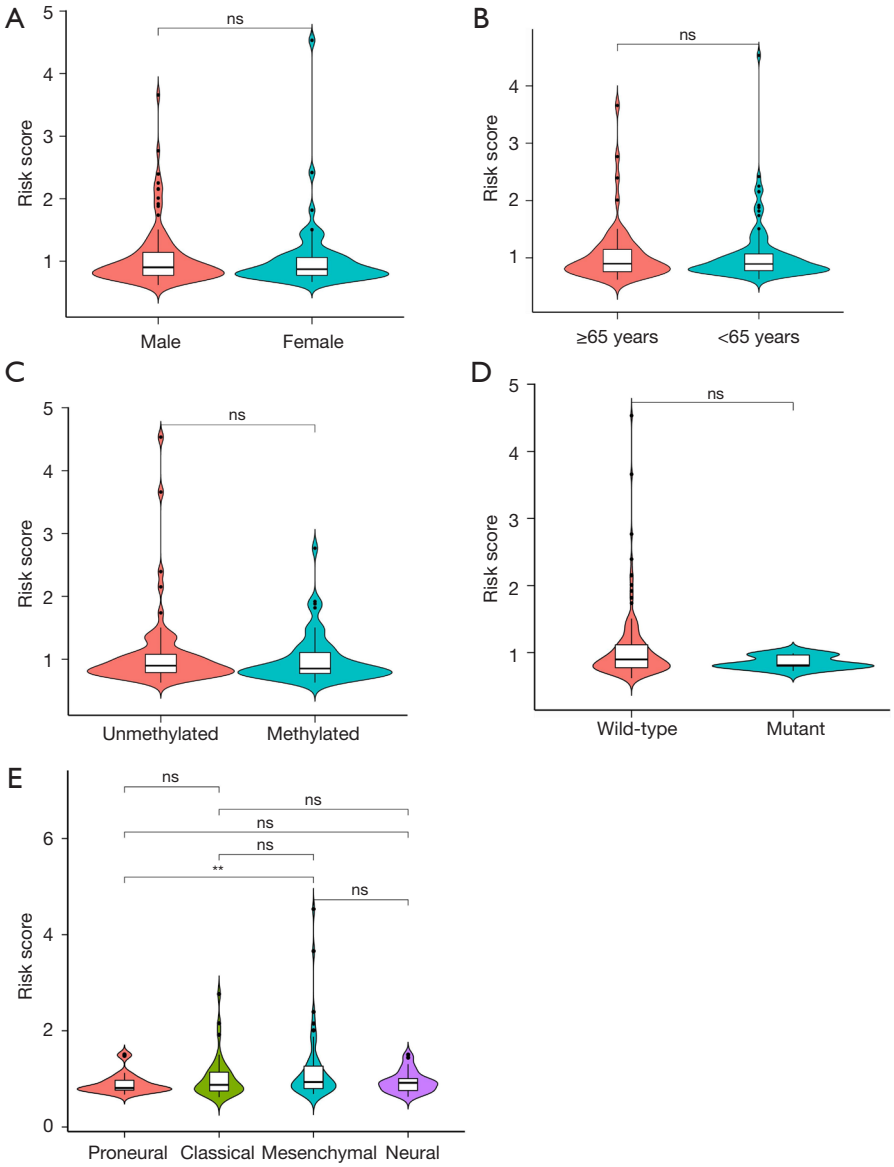

Figure 3 Differences in risk scores for clinical characteristics. (A-D) The correlations between the risk score and sex, age, MGMT status, and IDH1 status were not significant (P>0.05). (E) Among the subtypes, the proneural subtypes had a significantly lower risk score than did the mesenchymal subtypes (P<0.05). **, P<0.01. IDH1, isocitrate dehydrogenase 1; MGMT, O6-methylguanine-DNA methyltransferase; ns, no significance.

mRNAs. Finally, a ceRNA network containing 3 lncRNAs, 29 miRNAs, and 69 mRNAs was constructed based on the genes (|cor| >0.5; P<0.05; *Figure 5A*).

The functions of the target genes of the lncRNA signature were further analyzed. GO functional enrichment results showed that the target genes were significantly associated with biological processes, such as regulation of neurotransmitter secretion, synaptic organization, modulation of chemical synaptic transmission, regulation of membrane potential, regulation of exocytosis, synaptic vesicle exocytosis, regulation of the synaptic vesicle cycle, and regulation of trans-synaptic signaling. In terms of cellular composition, target genes were significantly related to the functions of synaptic membranes, presynaptic membranes, transport complexes, postsynaptic density, distal axons, neuron-to-neuron synapses, postsynaptic

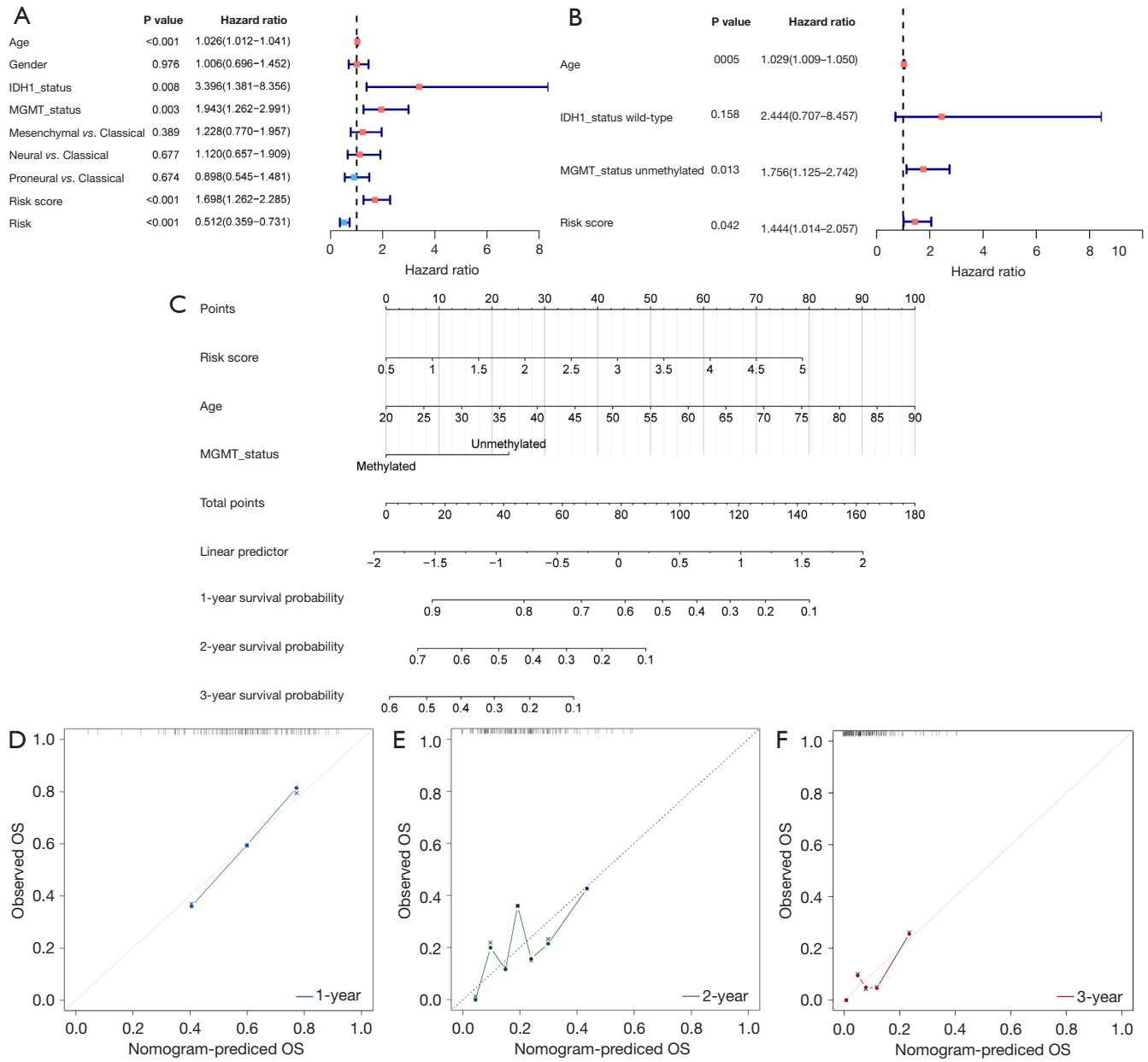

Figure 4 Using the lncRNA signature as an independent prognostic factor and construction of the nomogram. (A,B) The risk score based on the angiogenesis-related lncRNA signature is a dependable independent prognostic factor for patients with GBM. (C) A predictive nomogram of patients with GBM based on the risk score, age, and MGMT status. (D-F) The calibration curve of the nomogram for predicting the 1- to 3-year survival rate of patients. IDH1, isocitrate dehydrogenase 1; GBM, glioblastoma multiforme; lncRNAs, long noncoding RNAs; MGMT, O6-methylguanine-DNA methyltransferase; OS, overall survival.

specialization, glutamatergic synapses, transmembrane transporter complexes, and ion channel complexes. In terms of molecular function, the target genes were significantly linked to voltage-gated channel activity, ion channel activity, cation channel activity, metal ion transmembrane transporter activity, syntaxin-1 binding, and passive transmembrane transporter activity (*Figure 5B*). KEGG analysis showed a significant correlation between target genes and myocardial contraction, hypertrophic cardiomyopathy, the mitogen-activated protein kinase

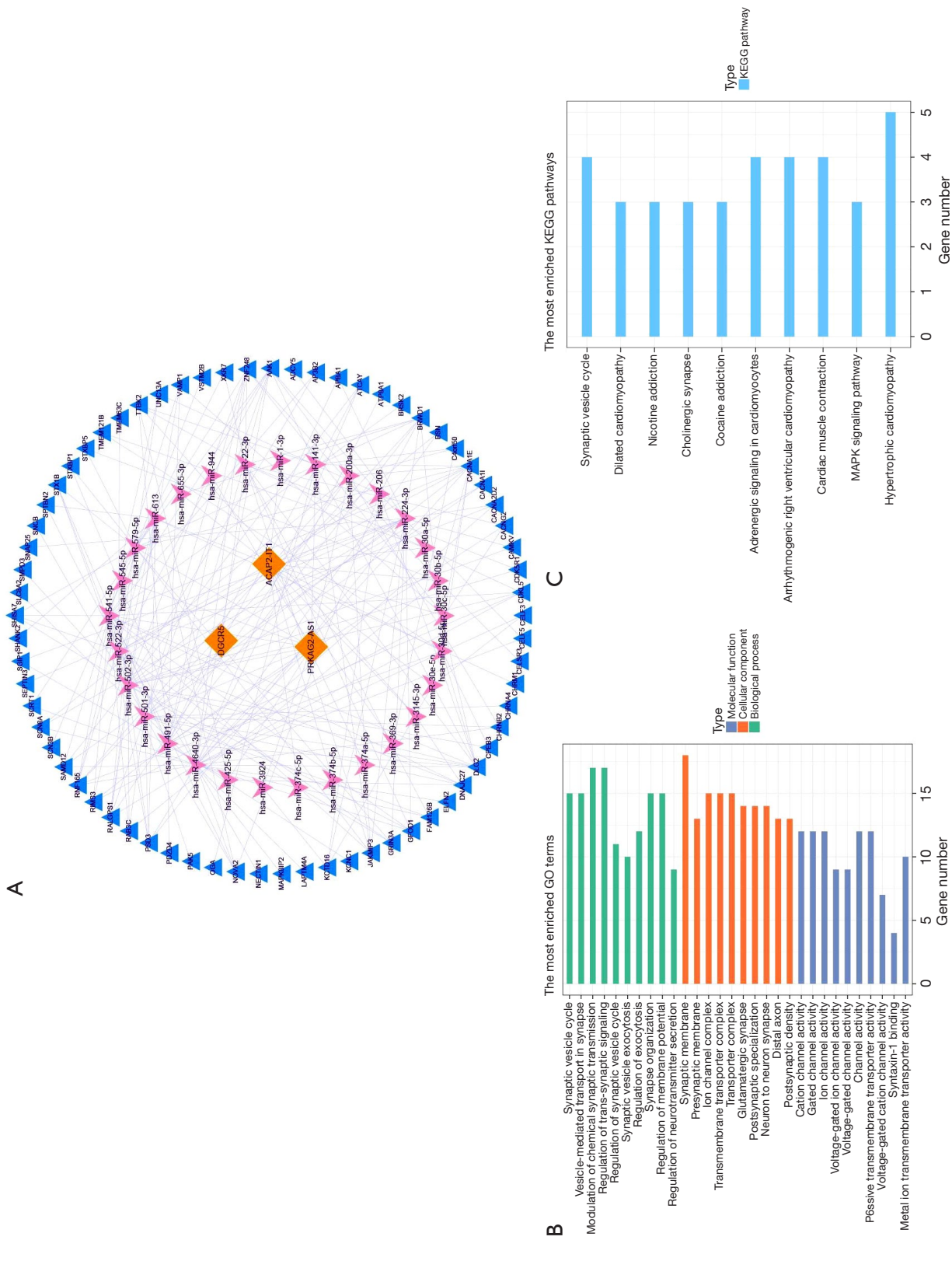

Figure 5 Construction of the ceRNA network of the angiogenesis-related lncRNA signature and functional analysis. (A) ceRNA network of the lncRNA signature. The blue triangle represents mRNA, the pink inverted triangle represents miRNA, and the yellow diamond represents lncRNA. (B) GO functional enrichment results of the target genes of the lncRNA signature. (C) KEGG pathway analysis results of the target genes of the lncRNA signature. ceRNA, competing endogenous RNA; GO, Gene Ontology; KEGG, Kyoto Encyclopedia of Genes and Genomes; lncRNAs, long noncoding RNAs; mRNA, messenger RNA; miRNA, microRNA.

(MAPK) signaling pathway, the synaptic vesicle cycle, hypertrophic cardiomyopathy, arrhythmogenic right ventricular cardiomyopathy, adrenergic signaling in cardiomyocytes, cocaine addiction, and cholinergic synapse (*Figure 5C*).

The lncRNA signature was associated with the immune microenvironment

The findings of the immune microenvironment analysis revealed that the immune score, stromal score, and combined ESTIMATE score of the 2 were higher in the high-risk group than in the low-risk group, indicating high immune cell infiltration in the high-risk group (*Figure 6A*). According to ssGSEA, the proportion of neutrophils, macrophages, immature dendritic cells (iDCs), natural killer (NK) CD56dim cells, and activated DCs (aDCs) were significantly different between the high- and low-risk groups ($P<0.05$; *Figure 6B*). In addition, only the proportion of resting NK cells was different between the groups in the CIBERSORT algorithm results ($P<0.05$; *Figure 6C*). The results analyzed in the "immunedeconv" package showed significant differences in the proportion of macrophage M2, uncharacterized cells, and macrophage/monocyte cells between the high- and low-risk groups ($P<0.05$; Figures S2A-S2C). A total of 10 immune/nonimmune cells were significantly different between the high- and low-risk groups based on online database xCell analysis; the differences were in megakaryocytes, keratinocytes, plasmacytoid dendritic cells (pDCs), macrophages, M2 macrophages, pro-B cells, memory B cells, NK cells, T helper type 1 (Th1 cells), and melanocytes ($P<0.05$; Figure S2D). Furthermore, the leukocyte fraction was significantly higher in the high-risk group than in the low-risk group ($P<0.05$; Figure S2E). These results suggest a powerful correlation between the 3-lncRNA signature and the immune microenvironment.

The lncRNA signature was associated with immunotherapy of PD-1-R

We assessed the correlation between the prognostic model and the expression values of immune checkpoint genes that could be used as indicators for predicting the immune response. The results demonstrated that only CD274, PDCD1LG2, LAG3, and PDCD1 immune checkpoint molecules were present in GBM samples; unfortunately, their expression did not show significant differences between the high- and low-risk groups (*Figure 7A*). In addition, the results of the differential assessment of immunotherapy sensitivity indicated no significant difference in the immune response in the high- and low-risk groups (*Figure 7B*). We further evaluated the response of the high- and low-risk groups to immunotherapy for PD-1 and CTLA4 and concluded that there was a significant difference in the sensitivity of immunotherapy for PD-1 between the high-risk group and low-risk group (*Figure 7C*).

The lncRNA signature could predict chemotherapy drug sensitivity

Analysis of differences in chemotherapy between high- and low-risk groups identified 28 drugs with significant differences in IC50 value, including OSI.906, cyclopamine, bosutinib, vinblastine, MG.132, cytarabine, AZD7762, A.770041, GSK269962A, FH535, ABT.888, pyrimethamine, salubrinal, lenalidomide, camptothecin, BIRB.0796, AS601245, NSC.87877, AICAR, MS.275, tipifarnib, cisplatin, nilotinib, dasatinib, KIN001.135, JNJ.26854165, axitinib, and A.443654. This result implies that these drugs may be potential chemotherapeutic agents for GBM (*Figure 8*).

Discussion

In recent years, the role of lncRNAs in the tumorigenesis and development of glioma has been gradually recognized. The function of lncRNAs is complicated and can be roughly divided into the following aspects: regulating the function of target proteins directly, regulating the stability and translation of long-stranded RNA molecules, affecting the inhibitory function of miRNAs, and regulating gene transcription (14). Many studies have shown that lncRNAs participate in the regulation of angiogenesis in glioma. Some lncRNAs can promote angiogenesis in glioma. lncRNA H19 promotes glioma angiogenesis via the miR-342-Wnt5a-beta-catenin axis (13). The lncRNA RPL34-AS1 promotes glioma angiogenesis by regulating the vascular endothelial growth factor A (VEGFA) signaling pathway (15). Other lncRNAs that have been reported to promote glioma angiogenesis include lncRNA PVT1 (16), lncRNA CCAT2 (17), and lncRNA NKILA (18).

Meanwhile, some lncRNAs show inhibitory effects on the angiogenesis of glioma. LncRNA SLC26A4-AS1 inhibits glioma angiogenesis by upregulating NPTX1 via nuclear factor kappa B subunit 1 (NFKB1) transcription

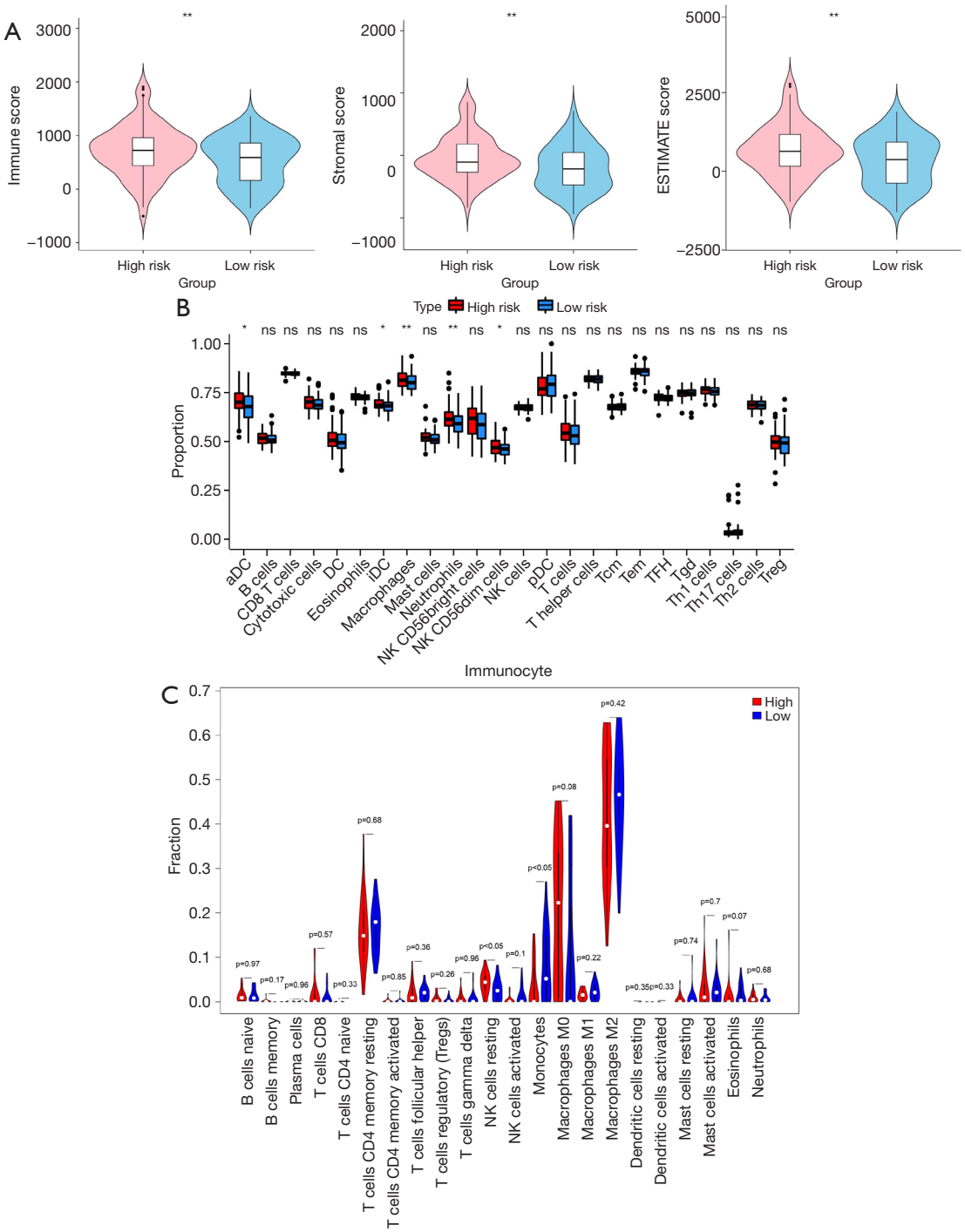

Figure 6 The relationship between the lncRNA signature and the immune microenvironment of GBM. (A) The immune score, stromal score, and combined ESTIMATE score were higher in the high-risk group than in the low-risk group. (B) According to ssGSEA, the proportion of neutrophils, macrophages, iDCs, NK CD56dim cells, and aDCs were significantly different between the high- and low-risk groups (P<0.05). (C) The proportion of resting NK cells was different between groups in the CIBERSORT algorithm results (P<0.05). *, P<0.05; **, P<0.01. aDC, activated DCs; DC, dendritic cell; ESTIMATE, Estimation of STromal and Immune cells in MAlignant Tumor tissues using Expression data; GBM, glioblastoma multiforme; iDC, immature dendritic cells; lncRNAs, long noncoding RNAs; NK, natural killer; ns, no significance; pDC, plasmacytoid dendritic cell; ssGSEA, single-sample gene set enrichment analysis; Tcm, central memory T cell; Tem, effector memory T cell; TFH, follicular helper T cell; Tgd, γ/δ T cell; Treg, T regulator cell.

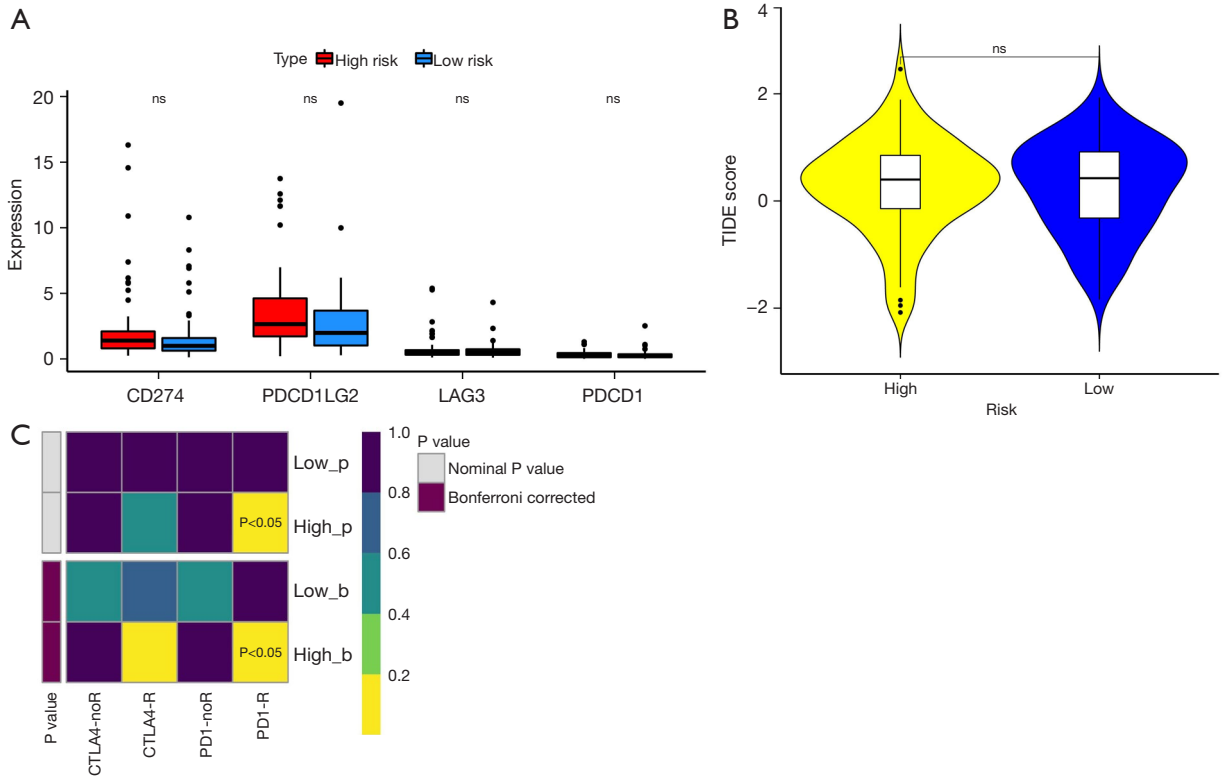

Figure 7 The relationship between the lncRNA signature and immunotherapy. (A) The expression of the immune checkpoint molecules CD274, PDCD1LG2, LAG3, and PDCD1 did not show significant differences between the high- and low-risk groups. (B) The TIDE score was not significantly different between the high- and low-risk groups. (C) The high-risk group possessed a higher sensitivity to PD-1 immunotherapy. ns, no significance. CTLA4, cytotoxic T-lymphocyte protein 4; lncRNAs, long noncoding RNAs; ns, no significance; PD-1, programmed cell death protein 1; TIDE, Tumor Immune Dysfunction and Exclusion.

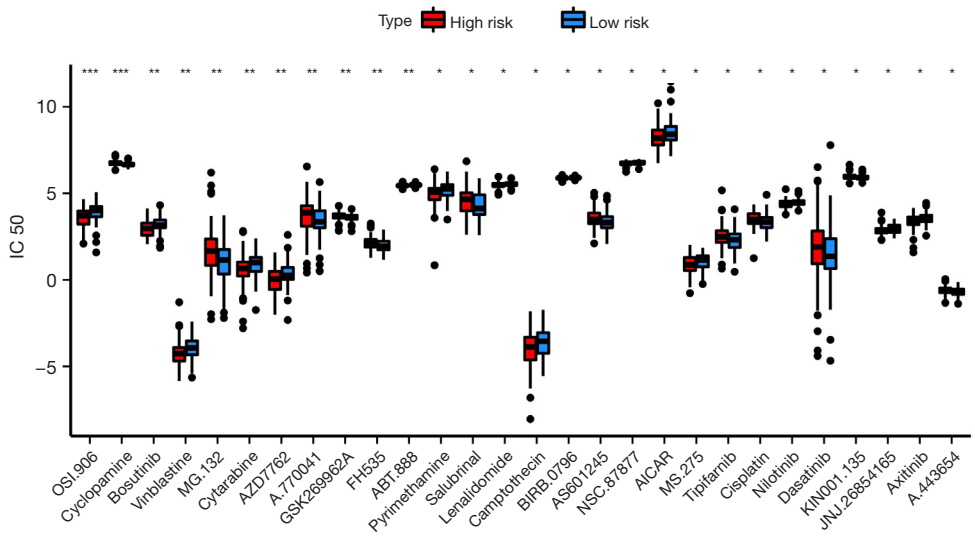

Figure 8 Drug sensitivity analysis of the high- and low-risk groups. *, P<0.05; **, P<0.01; ***, P<0.001.

factor (19). Since lncRNAs play an important role in the angiogenesis of glioma, they are considered potential targets for glioma therapy. It has been reported that the knockdown of lncRNA H19 can inhibit the proliferation, migration, and angiogenesis of glioma cells (13). Similar results have also been shown in other studies (15,17). In addition to participating in the regulation of glioma angiogenesis, lncRNAs are also related to the prognosis of patients with glioma. It has been shown that lncRNAs PVT1 and HAR1A can be used as prognostic biomarkers to indicate therapy outcomes for diffuse glioma patients (20). Some researchers constructed risk models based on immune-related lncRNAs. The results showed that the lncRNA-based risk model could be used to evaluate the prognosis of patients with glioma and predict the efficacy of immunotherapy (21).

In the present study, 3 AR-DElncRNAs (DGCR5, PRKAG2-AS1, and ACAP2-IT1) that significantly associated with the prognosis of patients with GBM were identified. lncRNA DGCR5 has been recognized as a potential tumor progression regulator. Abnormal expression of DGCR5 regulates the progression of digestive cancers by affecting cancer cell proliferation, aggression, metastasis, and drug resistance (22). In addition, DGCR5 also plays an important role in glioma. Some studies have shown that DGCR5 is significantly associated with the prognosis of patients with glioma and participates in the regulation of the immune response, immune infiltration, and cell proliferation of glioma (23,24). LncRNA PRKAG2-AS1 was reported to be a prognosis-related factor in patients with hepatocellular carcinoma (HCC) (25). Targeting PRKAG2-AS1 can significantly inhibit proliferation, migration, and invasion in HCC cells (25). LncRNA ACAP2-IT1 seems to be related to the regulation of N6-methyladenosine, which plays an important role in carcinogenesis and cancer inhibition (26). According to the results of the present study, DGCR5, PRKAG2-AS1, and ACAP2-IT1 are angiogenesis-related and are significantly associated with the OS of patients with GBM. This finding suggests that these 3 lncRNAs may provide potential therapeutic targets for further research on the antiangiogenic therapy of GBM.

We further established a risk model based on the 3 identified AR-DElncRNAs (DGCR5, PRKAG2-AS1, and ACAP2-IT1) and validated it. The results showed the good efficacy of the risk model. We then used the risk model to predict the prognosis of GBM with different clinicopathological characteristics. The results showed that the proneural subtypes had a significantly lower risk score than did the mesenchymal subtypes. The proneural subtype GBM has neuronal differentiation, which is common in young adults. The molecular pathological features of proneural GBM are IDH, TP53 mutations, and positivity for the glioma CpG island methylator phenotype (G-CIMP) and normal epidermal growth factor receptor (EGFR), PTEN, and Notch signaling. In contrast, mesenchymal GBM has mesenchymal differentiation, which is common in older adults. The molecular pathological features of mesenchymal GBM are abnormal EGFR amplification, PTEN loss, NF1 mutations, and Akt signaling (27). Compared with the mesenchymal subtype, the outcome of the proneural subtype is better (27), which is consistent with the risk score and proves the accuracy of the risk model.

To further investigate the regulatory mechanism of the lncRNA signature in GBM, we constructed a lncRNA signature–related ceRNA network, and 29 miRNAs were involved in this network. Among these miRNAs, miR-22-3p, miR-141-3p, miR-206, miR-30a-5p, miR-30b-5p, miR-491-5p, miR-655-3p, and miR-944 have been confirmed to be closely related to the progression, angiogenesis, radioresistance, and chemoresistance of glioma (28-35). Ten lncRNA signature-related pathways were identified using pathway enrichment analysis. Among them, the MAPK pathway has been confirmed to be closely related to angiogenesis, invasion, proliferation, and migration of glioma (36-38). These results indirectly link these AR-DElncRNAs to angiogenesis. However, direct evidence of the involvement of these lncRNAs in angiogenesis regulation is still lacking. The effects of these lncRNAs, miRNAs, and their target genes in the ceRNA network on glioma need to be further studied.

The GBM microenvironment contains infiltrating and resident immune cells, such as microglia, peripheral macrophages, myeloid-derived suppressor cells (MDSCs), leukocytes, $CD4^+$ T cells, and T regulator cells (Tregs), which have a crucial role in glioma growth, metastasis, and response to treatment (39). In the present study, although the results of various analysis methods were different in the types of immune cells, in general, the immune cell infiltration in the high-risk group was higher than that of the low-risk group. Notably, the CIBERSORT algorithm results showed that the proportion of NK resting cells was higher in the high-risk group than in the low-risk group. Some studies have confirmed that infiltrating NK cells in glioma tissues are nonfunctional, possibly due to contact with immunosuppressive cells, such as glioma-

associated microglia, macrophages (GAMs), MDSCs, and Tregs (39,40). These cells inhibit the activities of NK cells by suppressing NKG2D expression and the production of interferon gamma (INF-γ) (39). Meanwhile, the proportion of macrophages was higher in the high-risk group than in the low-risk group. Macrophages and microglia are the predominant immune population in gliomas and can constitute up to 30–50% of the total cellular composition (41). GAMs have been shown to engage in reciprocal interactions with neoplastic tumor cells to promote tumor growth and progression (42). The number of GAMs is higher in high-grade than in low-grade glioma and is generally a negative prognostic factor for survival (41). These results suggest that the risk model can help evaluate the tumor immune microenvironment of patients with GBM.

Our results showed that the high-risk group possessed a higher sensitivity to PD-1-R immunotherapy than did the low-risk group. Tumor-associated macrophages (TAMs) express PD-1. The expression of PD-1 on TAMs increases with tumor progression and correlates negatively with phagocytic activity against tumor cells. Blockade of PD-1/programmed death-ligand 1 (PD-L1) *in vivo* reduces tumor growth and increases survival in mouse models of cancer (43). Considering the higher proportion of macrophages in the high-risk group, this may be one of the mechanisms by which the high-risk group has a higher sensitivity to PD-1R immunotherapy compared to the low-risk group.

Finally, we analyzed the differences in chemotherapy drug sensitivity between the high- and low-risk groups. These results may provide valuable information for drug selection during the chemotherapy of GBM. However, the effectiveness of these drugs for GBM warrants further basic and clinical study validation.

There are a few limitations in our research. Our predictions and validation were conducted using bioinformatics technologies, and we did not conduct clinical research with our patient tissue samples. In addition, further experiments *in vivo* and *in vitro* were absent, which should be addressed in our future research. Despite these limitations, the results in this study were accurate and acquired after extensive data analysis. Our results provide a new research direction that can progress our understanding of the mechanism of glioblastoma.

In conclusion, we developed and validated an angiogenesis-related lncRNA signature for predicting the prognosis of patients with GBM. Moreover, the novel signature could be applied for therapeutic response prediction during the treatment of these patients.

Acknowledgments

Funding: This study was funded by the Key Research and Development Plan of Shaanxi Province, China (No. 2021SF-298).

Footnote

Reporting Checklist: The authors have completed the TRIPOD reporting checklist. Available at https://tcr.amegroups.com/article/view/10.21037/tcr-22-1592/rc

Peer Review File: Available at https://tcr.amegroups.com/article/view/10.21037/tcr-22-1592/prf

Conflicts of Interest: All authors have completed the ICMJE uniform disclosure form (available at https://tcr.amegroups.com/article/view/10.21037/tcr-22-1592/coif). The authors have no conflicts of interest to declare.

Ethical Statement: The authors are accountable for all aspects of the work in ensuring that questions related to the accuracy or integrity of any part of the work are appropriately investigated and resolved. The study was conducted in accordance with the Declaration of Helsinki (as revised in 2013).

References

1. Louis DN, Perry A, Reifenberger G, et al. The 2016 World Health Organization Classification of Tumors of the Central Nervous System: a summary. Acta Neuropathol 2016;131:803-20.
2. Shergalis A, Bankhead A 3rd, Luesakul U, et al. Current Challenges and Opportunities in Treating Glioblastoma.

Pharmacol Rev 2018;70:412-45.
3. Wen PY, Kesari S. Malignant gliomas in adults. N Engl J Med 2008;359:492-507.
4. Peshes-Yeloz N, Ungar L, Wohl A, et al. Role of Klotho Protein in Tumor Genesis, Cancer Progression, and Prognosis in Patients with High-Grade Glioma. World Neurosurg 2019;130:e324-32.
5. Wong ML, Prawira A, Kaye AH, et al. Tumour angiogenesis: its mechanism and therapeutic implications in malignant gliomas. J Clin Neurosci 2009;16:1119-30.
6. Parmar D, Apte M. Angiopoietin inhibitors: A review on targeting tumor angiogenesis. Eur J Pharmacol 2021;899:174021.
7. Ahir BK, Engelhard HH, Lakka SS. Tumor Development and Angiogenesis in Adult Brain Tumor: Glioblastoma. Mol Neurobiol 2020;57:2461-78.
8. Schulte JD, Aghi MK, Taylor JW. Anti-angiogenic therapies in the management of glioblastoma. Chin Clin Oncol 2021;10:37.
9. Zhao W, Shan B, He D, et al. Recent Progress in Characterizing Long Noncoding RNAs in Cancer Drug Resistance. J Cancer 2019;10:6693-702.
10. Zhang X, Niu W, Mu M, et al. Long non-coding RNA LPP-AS2 promotes glioma tumorigenesis via miR-7-5p/EGFR/PI3K/AKT/c-MYC feedback loop. J Exp Clin Cancer Res 2020;39:196.
11. Yang H, Chen W, Jiang G, et al. Long non-coding RNA EWSAT1 contributes to the proliferation and invasion of glioma by sponging miR-152-3p. Oncol Lett 2020;20:1846-54.
12. Li B, Lu X, Ma C, et al. Long non-coding RNA NEAT1 promotes human glioma tumor progression via miR-152-3p/CCT6A pathway. Neurosci Lett 2020;732:135086.
13. Zhou Q, Liu ZZ, Wu H, et al. LncRNA H19 Promotes Cell Proliferation, Migration, and Angiogenesis of Glioma by Regulating Wnt5a/β-Catenin Pathway via Targeting miR-342. Cell Mol Neurobiol 2022;42:1065-77.
14. Li D, Zhang Z, Xia C, et al. Non-Coding RNAs in Glioma Microenvironment and Angiogenesis. Front Mol Neurosci 2021;14:763610.
15. Zhang D, Jiang H, Ye J, et al. A novel lncRNA, RPL34-AS1, promotes proliferation and angiogenesis in glioma by regulating VEGFA. J Cancer 2021;12:6189-97.
16. Bi Y, Ji J, Zhou Y. LncRNA-PVT1 indicates a poor prognosis and promotes angiogenesis via activating the HNF1B/EMT axis in glioma. J Cancer 2021;12:5732-44.
17. Sun SL, Shu YG, Tao MY. LncRNA CCAT2 promotes angiogenesis in glioma through activation of VEGFA signalling by sponging miR-424. Mol Cell Biochem 2020;468:69-82.
18. Chen Z, Li S, Shen L, et al. NF-kappa B interacting long noncoding RNA enhances the Warburg effect and angiogenesis and is associated with decreased survival of patients with gliomas. Cell Death Dis 2020;11:323.
19. Li H, Yan R, Chen W, et al. Long non coding RNA SLC26A4-AS1 exerts antiangiogenic effects in human glioma by upregulating NPTX1 via NFKB1 transcriptional factor. FEBS J 2021;288:212-28.
20. Zou H, Wu LX, Yang Y, et al. lncRNAs PVT1 and HAR1A are prognosis biomarkers and indicate therapy outcome for diffuse glioma patients. Oncotarget 2017;8:78767-80.
21. Wang X, Gao M, Ye J, et al. An Immune Gene-Related Five-lncRNA Signature for to Predict Glioma Prognosis. Front Genet 2020;11:612037.
22. Hu C, Xu W, Wang B, et al. Critical Functions of lncRNA DGCR5 in Cancers of the Digestive System. Curr Pharm Des 2021;27:4147-51.
23. Wu X, Hou P, Qiu Y, et al. Large-Scale Analysis Reveals the Specific Clinical and Immune Features of DGCR5 in Glioma. Onco Targets Ther 2020;13:7531-43.
24. He Z, Long J, Yang C, et al. LncRNA DGCR5 plays a tumor-suppressive role in glioma via the miR-21/Smad7 and miR-23a/PTEN axes. Aging (Albany NY) 2020;12:20285-307.
25. Ou Y, Deng Y, Wang H, et al. Targeting Antisense lncRNA PRKAG2-AS1, as a Therapeutic Target, Suppresses Malignant Behaviors of Hepatocellular Carcinoma Cells. Front Med (Lausanne) 2021;8:649279.
26. Zheng J, Guo J, Cao B, et al. Identification and validation of lncRNAs involved in m6A regulation for patients with ovarian cancer. Cancer Cell Int 2021;21:363.
27. Olar A, Aldape KD. Using the molecular classification of glioblastoma to inform personalized treatment. J Pathol 2014;232:165-77.
28. Wang B, Wang K, Jin T, et al. NCK1-AS1 enhances glioma cell proliferation, radioresistance and chemoresistance via miR-22-3p/IGF1R ceRNA pathway. Biomed Pharmacother 2020;129:110395.
29. Yu M, Yi B, Zhou W, et al. Linc00475 promotes the progression of glioma by regulating the miR-141-3p/YAP1 axis. J Cell Mol Med 2021;25:463-72.
30. Wang D, Yang T, Liu J, et al. Propofol Inhibits the Migration and Invasion of Glioma Cells by Blocking the PI3K/AKT Pathway Through miR-206/ROCK1 Axis. Onco Targets Ther 2020;13:361-70.

31. Zhao P, Wang M, An J, et al. A positive feedback loop of miR-30a-5p-WWP1-NF-κB in the regulation of glioma development. Int J Biochem Cell Biol 2019;112:39-49.
32. Zhang D, Liu Z, Zheng N, et al. MiR-30b-5p modulates glioma cell proliferation by direct targeting MTDH. Saudi J Biol Sci 2018;25:947-52.
33. Li W, Soufiany I, Lyu X, et al. SP1-upregulated LBX2-AS1 promotes the progression of glioma by targeting the miR-491-5p/LIF axis. J Cancer 2021;12:6989-7002.
34. Xin J, Zhao YH, Zhang XY, et al. LncRNA NFIA-AS2 promotes glioma progression through modulating the miR-655-3p/ZFX axis. Hum Cell 2020;33:1273-80.
35. Jiang J, Lu J, Wang X, et al. Glioma stem cell-derived exosomal miR-944 reduces glioma growth and angiogenesis by inhibiting AKT/ERK signaling. Aging (Albany NY) 2021;13:19243-59.
36. Wang P, Hao X, Li X, et al. Curcumin inhibits adverse psychological stress-induced proliferation and invasion of glioma cells via down-regulating the ERK/MAPK pathway. J Cell Mol Med 2021;25:7190-203.
37. Tang F, Wang H, Chen E, et al. LncRNA-ATB promotes TGF-β-induced glioma cells invasion through NF-κB and P38/MAPK pathway. J Cell Physiol 2019;234(12):23302-14.
38. Wang A, Meng M, Zhao X, et al. Long non-coding RNA ENST00462717 suppresses the proliferation, survival, and migration by inhibiting MDM2/MAPK pathway in glioma. Biochem Biophys Res Commun 2017;485:513-21.
39. Gieryng A, Pszczolkowska D, Walentynowicz KA, et al. Immune microenvironment of gliomas. Lab Invest 2017;97:498-518.
40. Fu W, Wang W, Li H, et al. Single-Cell Atlas Reveals Complexity of the Immunosuppressive Microenvironment of Initial and Recurrent Glioblastoma. Front Immunol 2020;11:835.
41. Wei J, Chen P, Gupta P, et al. Immune biology of glioma-associated macrophages and microglia: functional and therapeutic implications. Neuro Oncol 2020;22:180-94.
42. Chen Z, Hambardzumyan D. Immune Microenvironment in Glioblastoma Subtypes. Front Immunol 2018;9:1004.
43. Gordon SR, Maute RL, Dulken BW, et al. PD-1 expression by tumour-associated macrophages inhibits phagocytosis and tumour immunity. Nature 2017;545:495-9.

Cite this article as: Zhang B, Cheng Y, Li R, Lian M, Guo S, Liang C. Development of a novel angiogenesis-related lncRNA signature to predict the prognosis and immunotherapy of glioblastoma multiforme. Transl Cancer Res 2023;12(1):13-30. doi: 10.21037/tcr-22-1592

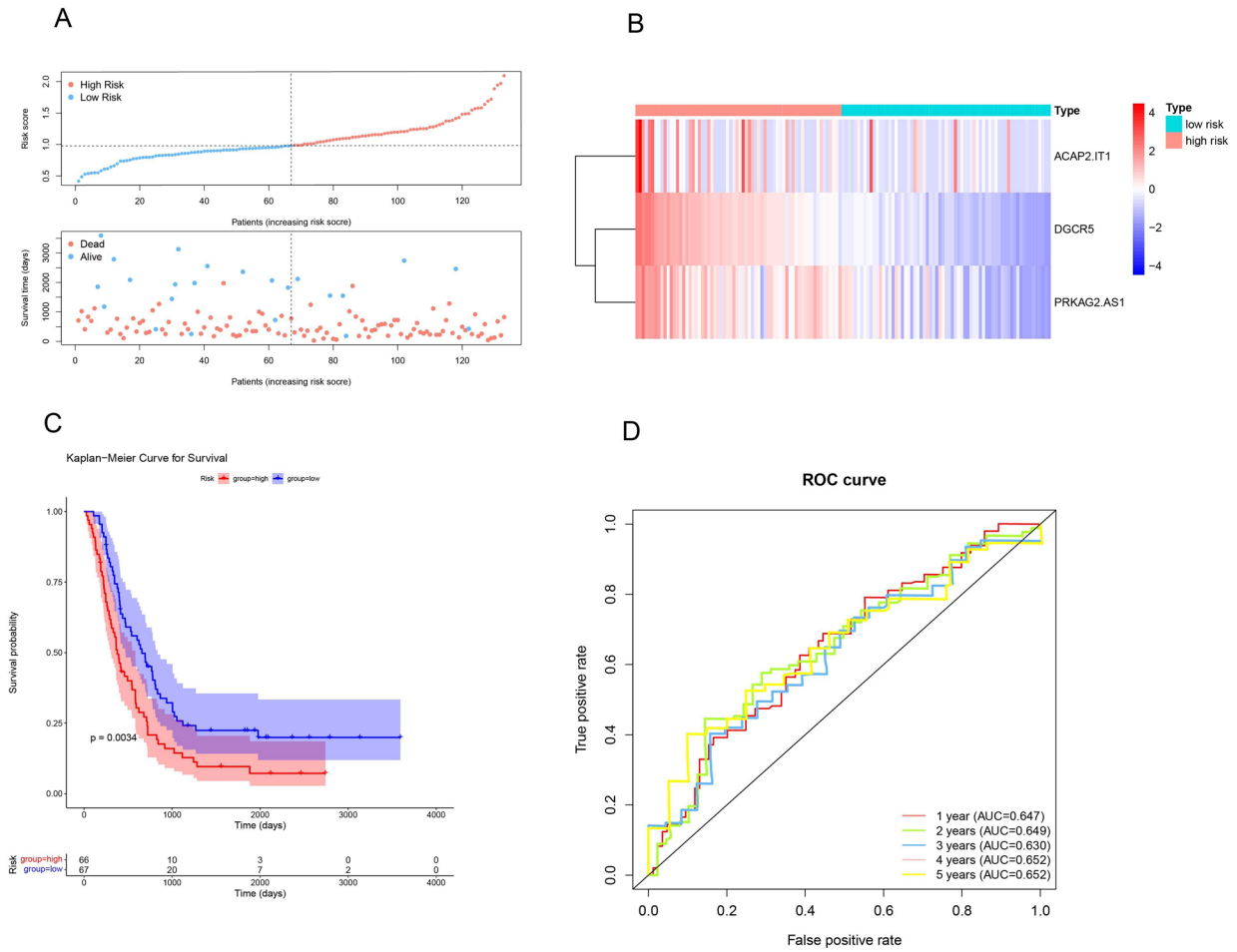

Figure S1 Validation of the angiogenesis-related lncRNA signature. (A-D) Validation of the angiogenesis-related lncRNA signature in the external validation set. AUC, area under the curve; lncRNAs, long noncoding RNAs; ROC, receiver operating characteristic.

https://dx.doi.org/10.21037/tcr-22-1592

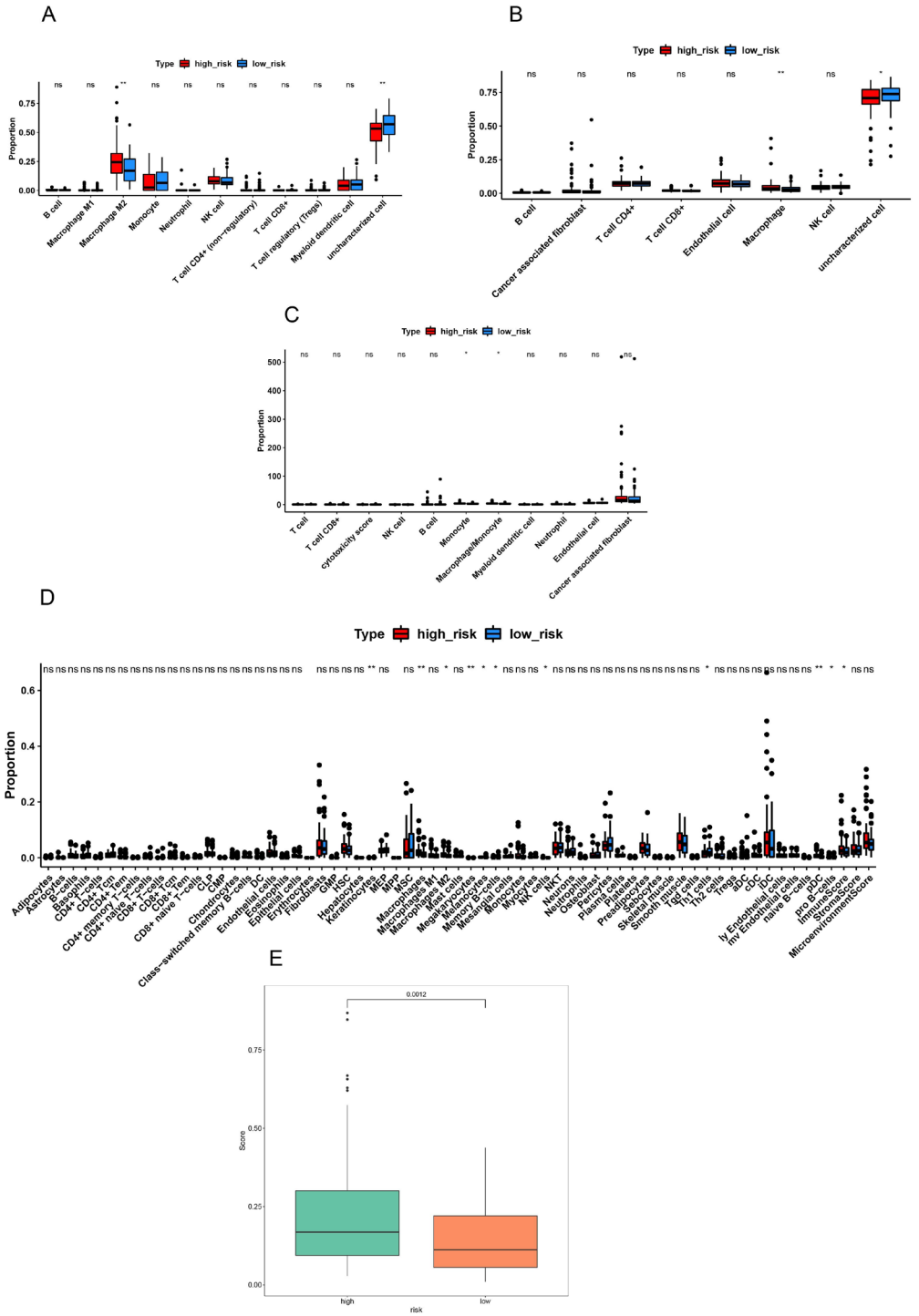

Figure S2 The relationship between the lncRNA signature and the immune microenvironment of GBM. (A-C) The results analyzed in the "immunedeconv" package showed significant differences in macrophage M2, uncharacterized cells, and macrophage/monocyte cells between the high- and low-risk groups (P<0.05). (D) Online database xCell analysis showed the difference in immune/nonimmune cells between the high- and low-risk groups (P<0.05). (E) The leukocyte fraction was significantly higher in the high-risk group than in the low-risk group (P<0.05). *, P<0.05; **, P<0.01. aDC, activated DCs; CLP, common lymphoid progenitor; CMP, common myeloid progenitors; cDC, conventional dendritic cell; DC, dendritic cell; GBM, glioblastoma multiforme; GMP, granulocyte-monocyte progenitor; HSC, hepatic stellate cell; iDC, immature dendritic cells; lncRNAs, long noncoding RNAs; ly, lymphatic; MEP, megakaryocyte erythroid progenitor; MPP, multipotent blood progenitors; MSC, mesenchymal stem cell; mv, microvascular; NK, natural killer; NKT, natural killer T; ns, no significance; pDC, plasmacytoid dendritic cell; Tcm, central memory T cell; Tem, effector memory T cell; Tgd, γ/δ T cell; Treg, T regulator cell.

https://dx.doi.org/10.21037/tcr-22-1592

Table S1 The clinical information of TCGA-GBM cohorts

ID	fustat	futime	Vital	Age, year	Gender	Grade	IDH status	MGMT promoter status	Karnofsky Performance Score	Original subtype	riskScore	Risk	Group	Chemo_status	Radio_status
TCGA-02-0047	1	448	Dead	78	Male	G4	WT	Unmethylated	80	Proneural	0.652851	Low	Testing	Untreated	Treated
TCGA-02-0055	1	76	Dead	62	Female	G4	WT	Unmethylated	80	Mesenchymal	1.439318	High	Testing	Treated	Treated
TCGA-02-2483	0	466	Alive	43	Male	G4	Mutant	Methylated	80	G-CIMP	0.188503	Low	Training	Treated	Treated
TCGA-02-2485	0	470	Alive	53	Male	G4	WT	Unmethylated	80	Classical	0.532921	Low	Training	Treated	Treated
TCGA-02-2486	1	618	Dead	64	Male	G4	WT	Unmethylated	80	Mesenchymal	1.522593	High	Training	Treated	Treated
TCGA-06-0125	1	1448	Dead	63	Female	G4	WT	Methylated	60	Classical	0.332571	Low	Training	Treated	Treated
TCGA-06-0129	1	1024	Dead	30	Male	G4	Mutant	Methylated	100	G-CIMP	0.365485	Low	Training	Treated	Treated
TCGA-06-0130	1	394	Dead	54	Male	G4	WT	Unmethylated	80	Mesenchymal	2.657	High	Training	Treated	Treated
TCGA-06-0132	1	771	Dead	49	Male	G4	WT	NA	NA	Neural	0.614776	Low	Training	Treated	Treated
TCGA-06-0138	1	737	Dead	43	Male	G4	WT	NA	80	Neural	1.399154	High	Training	Treated	Treated
TCGA-06-0139	1	362	NA	40	Male	NA	NA	NA	NA	NA	1.300784	High	Training	NA	NA
TCGA-06-0141	1	313	Dead	62	Male	G4	WT	Unmethylated	80	Mesenchymal	1.666885	High	Testing	Treated	Treated
TCGA-06-0152	1	375	Dead	NA	NA	NA	NA	NA	NA	NA	2.295225	High	Training	Treated	Treated
TCGA-06-0156	1	178	Dead	57	Male	G4	Mutant	NA	NA	Proneural	1.485481	High	Training	Treated	Treated
TCGA-06-0157	1	97	Dead	63	Female	G4	WT	NA	40	Classical	0.751434	Low	Testing	Untreated	Treated
TCGA-06-0158	1	329	Dead	73	Male	G4	WT	NA	80	Classical	0.891303	Low	Testing	Treated	Treated
TCGA-06-0168	1	598	Dead	59	Female	G4	WT	NA	100	Mesenchymal	1.931492	High	Testing	Treated	Treated
TCGA-06-0171	1	399	Dead	NA	NA	NA	NA	NA	NA	NA	1.4283	High	Training	Treated	Treated
TCGA-06-0174	1	98	Dead	54	Male	G4	WT	NA	80	Proneural	0.48875	Low	Training	Treated	Treated
TCGA-06-0178	1	2681	Dead	38	Male	G4	Mutant	NA	NA	Neural	0.128263	Low	Training	Treated	Treated
TCGA-06-0184	1	2126	Dead	63	Male	G4	WT	NA	80	Mesenchymal	0.866013	Low	Training	Treated	Treated
TCGA-06-0187	1	828	Dead	69	Male	G4	WT	NA	60	Classical	2.225689	High	Training	Treated	Treated
TCGA-06-0190	1	317	Dead	NA	NA	NA	NA	NA	NA	NA	3.610125	High	Testing	Treated	Treated
TCGA-06-0210	1	225	Dead	NA	NA	NA	NA	NA	NA	NA	1.777131	High	Training	Untreated	Treated
TCGA-06-0211	1	360	Dead	NA	NA	NA	NA	NA	NA	NA	0.935453	Low	Training	Treated	Treated
TCGA-06-0219	1	22	Dead	67	Male	G4	WT	NA	NA	Neural	1.061894	Low	Training	Untreated	Untreated
TCGA-06-0221	1	603	Dead	NA	NA	NA	NA	NA	NA	NA	0.399837	Low	Training	Treated	Treated
TCGA-06-0238	1	405	Dead	46	Male	G4	WT	NA	80	Proneural	1.050777	Low	Training	Treated	Treated
TCGA-06-0644	1	384	Dead	71	Male	G4	WT	NA	80	Mesenchymal	4.145977	High	Training	Treated	Treated
TCGA-06-0645	1	175	Dead	55	Female	G4	WT	NA	NA	Mesenchymal	1.192949	High	Training	Untreated	Untreated
TCGA-06-0646	1	175	Dead	60	Male	G4	WT	NA	80	Proneural	2.316383	High	Training	Treated	Treated
TCGA-06-0649	1	64	Dead	73	Female	G4	WT	NA	NA	Neural	1.799702	High	Training	Untreated	Untreated
TCGA-06-0686	1	432	Dead	53	Male	G4	WT	NA	NA	Proneural	1.042948	Low	Training	Treated	Treated
TCGA-06-0743	1	803	Dead	69	Male	G4	WT	NA	100	Classical	0.587472	Low	Training	Treated	Treated
TCGA-06-0744	1	1426	Dead	66	Male	G4	WT	NA	80	Classical	0.261297	Low	Training	Treated	Treated
TCGA-06-0745	1	239	Dead	59	Male	G4	WT	NA	80	Proneural	1.980193	High	Training	Treated	Treated
TCGA-06-0747	1	82	Dead	53	Male	G4	WT	NA	80	Classical	1.717002	High	Training	Treated	Treated
TCGA-06-0749	1	82	Dead	50	Male	G4	WT	NA	NA	Neural	0.681388	Low	Training	Treated	Treated
TCGA-06-0750	1	28	Dead	43	Male	G4	WT	NA	80	Mesenchymal	2.488401	High	Testing	Untreated	Untreated
TCGA-06-0878	0	218	Alive	74	Male	G4	WT	Unmethylated	80	Mesenchymal	2.340513	High	Training	Treated	Treated
TCGA-06-0882	1	632	Dead	30	Male	G4	WT	Unmethylated	60	Neural	1.137865	High	Training	Treated	Treated
TCGA-06-1804	1	414	Dead	81	Female	G4	WT	Methylated	NA	Classical	0.878216	Low	Training	Untreated	Untreated
TCGA-06-2557	1	33	Dead	76	Male	G4	WT	Unmethylated	40	Mesenchymal	0.819007	Low	Training	Untreated	Untreated
TCGA-06-2558	1	380	Dead	75	Female	G4	WT	Unmethylated	60	Proneural	1.161375	High	Training	NA	Treated
TCGA-06-2559	1	150	Dead	83	Male	G4	WT	Methylated	60	Proneural	0.416095	Low	Training	Treated	Treated
TCGA-06-2561	1	537	Dead	53	Female	G4	WT	Unmethylated	80	Mesenchymal	2.49757	High	Testing	Treated	Treated
TCGA-06-2562	1	382	Dead	81	Male	G4	WT	Unmethylated	80	Mesenchymal	2.527492	High	Testing	Treated	Treated
TCGA-06-2563	0	932	Alive	72	Female	G4	WT	Methylated	80	Classical	0.527632	Low	Training	Treated	Treated
TCGA-06-2564	0	181	Alive	50	Male	G4	WT	Unmethylated	100	Classical	1.434918	High	Training	NA	Treated
TCGA-06-2565	1	506	Dead	59	Male	G4	WT	Methylated	100	Classical	0.394537	Low	Training	Treated	Treated
TCGA-06-2567	1	133	Dead	65	Male	G4	WT	Methylated	80	Neural	1.248933	High	Training	Treated	Treated
TCGA-06-2569	0	13	Alive	24	Female	G4	WT	Unmethylated	80	Mesenchymal	0.118833	Low	Training	NA	NA
TCGA-06-2570	0	958	Alive	21	Female	G4	Mutant	Methylated	100	G-CIMP	0.297724	Low	Testing	Treated	Treated
TCGA-06-5408	1	357	Dead	54	Female	G4	WT	Unmethylated	80	Classical	1.694289	High	Training	Treated	Treated
TCGA-06-5410	1	108	Dead	72	Female	G4	WT	Methylated	60	Mesenchymal	1.812995	High	Testing	Untreated	Untreated
TCGA-06-5411	1	254	Dead	51	Male	G4	WT	Unmethylated	80	Neural	1.247855	High	Training	Treated	Treated
TCGA-06-5412	1	138	Dead	78	Female	G4	WT	Methylated	80	Mesenchymal	2.91876	High	Testing	Treated	Treated
TCGA-06-5413	0	268	Alive	67	Male	G4	WT	Unmethylated	60	Neural	1.162171	Low	Training	Treated	Treated
TCGA-06-5414	0	273	Alive	61	Male	G4	WT	Unmethylated	80	Classical	1.9562	High	Training	Treated	Treated
TCGA-06-5416	0	204	Alive	23	Female	G4	NA	Unmethylated	80	Proneural	0.615482	Low	Testing	Treated	Treated
TCGA-06-5417	0	155	Alive	45	Female	G4	Mutant	Methylated	80	G-CIMP	0.282754	Low	Training	Treated	Treated
TCGA-06-5418	1	83	Dead	75	Female	G4	WT	Unmethylated	60	Mesenchymal	2.750282	High	Testing	Untreated	Untreated
TCGA-06-5856	1	114	Dead	58	Male	G4	WT	Unmethylated	NA	Classical	1.127737	Low	Training	Untreated	Untreated
TCGA-06-5858	0	187	Alive	45	Female	G4	WT	Unmethylated	100	Mesenchymal	0.496713	Low	Training	Treated	Treated
TCGA-06-5859	0	139	Alive	63	Male	G4	WT	Unmethylated	40	Neural	1.648324	High	Training	Treated	Treated
TCGA-08-0386	1	548	Dead	74	Male	G4	WT	NA	80	Neural	1.372743	High	Training	Treated	Treated
TCGA-12-0616	1	448	Dead	36	Female	G4	WT	NA	100	Proneural	0.709492	Low	Training	Treated	Treated
TCGA-12-0618	1	395	Dead	49	Male	G4	WT	NA	60	Proneural	0.793597	Low	Testing	Treated	Treated
TCGA-12-0619	1	1062	Dead	60	Male	G4	WT	NA	80	Mesenchymal	1.411514	High	Training	Treated	Treated
TCGA-12-0821	1	323	Dead	62	Male	G4	WT	Unmethylated	60	Neural	0.741342	Low	Training	Treated	Treated
TCGA-12-1597	1	675	Dead	62	Female	G4	WT	Unmethylated	80	Proneural	0.195243	Low	Training	Treated	Treated
TCGA-12-3650	1	333	Dead	46	Male	G4	WT	Unmethylated	80	Proneural	0.208942	Low	Training	Treated	Treated
TCGA-12-3652	1	1062	Dead	60	Male	G4	WT	Unmethylated	80	Classical	0.05865	Low	Training	Treated	Treated
TCGA-12-3653	1	442	Dead	34	Female	G4	WT	Unmethylated	80	Classical	0.817901	Low	Training	Treated	Treated
TCGA-12-5295	1	454	Dead	60	Female	G4	WT	Methylated	NA	Neural	0.497404	Low	Training	Treated	Treated
TCGA-12-5299	1	98	Dead	56	Female	G4	WT	Unmethylated	80	Classical	2.112583	High	Training	Treated	Treated
TCGA-14-0736	1	460	Dead	NA	NA	NA	NA	NA	NA	NA	1.362956	High	Training	Treated	Treated
TCGA-14-0781	1	29	Dead	49	Male	G4	WT	Unmethylated	NA	Mesenchymal	3.185952	High	Testing	Treated	Untreated
TCGA-14-0787	1	68	Dead	69	Male	G4	WT	Methylated	60	Classical	1.107037	Low	Testing	Treated	Untreated
TCGA-14-0789	1	342	Dead	54	Male	G4	WT	Methylated	40	Mesenchymal	2.359521	High	Training	Treated	Treated
TCGA-14-0790	1	419	Dead	64	Female	G4	WT	Methylated	60	Classical	0.57714	Low	Testing	Treated	Treated
TCGA-14-0817	1	164	Dead	69	Female	G4	WT	Unmethylated	60	Neural	0.538421	Low	Testing	Treated	NA
TCGA-14-0871	1	880	Dead	74	Female	G4	WT	Unmethylated	60	Mesenchymal	0.002077	Low	Training	Treated	Treated
TCGA-14-1034	1	485	Dead	NA	NA	NA	NA	NA	NA	NA	2.373282	High	Training	Treated	Treated
TCGA-14-1402	1	975	Dead	NA	NA	NA	NA	NA	NA	NA	1.201044	High	Training	Treated	Treated
TCGA-14-1823	1	543	Dead	58	Female	G4	WT	Methylated	80	Mesenchymal	1.176802	High	Training	Treated	Treated
TCGA-14-1825	1	232	Dead	70	Male	G4	WT	Unmethylated	80	Proneural	1.158547	High	Testing	Treated	Treated
TCGA-14-1829	0	218	Alive	57	Male	G4	WT	Unmethylated	60	Neural	0.748218	Low	Training	Treated	Treated
TCGA-14-2554	1	532	Dead	52	Female	G4	WT	Unmethylated	60	Neural	0.841839	Low	Training	Treated	Treated
TCGA-15-0742	1	419	Dead	65	Male	G4	WT	NA	80	Classical	1.222115	High	Testing	Treated	Treated
TCGA-15-1444	1	1537	Dead	21	Male	G4	Mutant	Methylated	NA	Proneural	0.274015	Low	Training	Treated	Treated
TCGA-16-0846	1	119	Dead	85	Male	G4	WT	Methylated	NA	Proneural	0.755751	Low	Training	Untreated	Untreated
TCGA-16-1045	1	883	Dead	49	Female	G4	WT	Methylated	NA	Mesenchymal	1.270922	High	Training	Treated	Treated
TCGA-19-0957	1	666	Dead	NA	NA	NA	NA	NA	NA	NA	1.280781	High	Training	Treated	Treated
TCGA-19-1389	1	141	Dead	NA	NA	NA	NA	NA	NA	NA	7.232813	High	Training	Treated	Treated
TCGA-19-1390	1	772	Dead	63	Female	G4	WT	Methylated	60	Proneural	0.409172	Low	Training	Untreated	Untreated
TCGA-19-1787	1	385	Dead	48	Male	G4	NA	Methylated	80	Mesenchymal	0.837618	Low	Training	Treated	Treated
TCGA-19-2619	0	294	Alive	55	Female	G4	WT	Methylated	40	Classical	0.958804	Low	Training	Treated	Treated
TCGA-19-2620	1	148	Dead	70	Male	G4	WT	Methylated	40	Neural	1.190592	Low	Training	Treated	Treated
TCGA-19-2624	1	5	Dead	51	Male	G4	WT	Unmethylated	NA	Proneural	1.668594	High	Training	Untreated	Untreated
TCGA-19-2625	1	124	Dead	76	Female	G4	WT	Unmethylated	NA	Classical	1.809246	High	Training	Untreated	Untreated
TCGA-19-2629	1	737	Dead	60	Male	G4	Mutant	Unmethylated	NA	G-CIMP	1.362137	High	Training	Treated	Treated
TCGA-19-4065	0	214	Alive	36	Male	G4	NA	Unmethylated	NA	NA	1.422923	High	Testing	Treated	Treated
TCGA-19-5960	1	455	Dead	56	Male	G4	WT	Unmethylated	80	Proneural	0.549375	Low	Training	Treated	Treated
TCGA-26-1442	0	953	Alive	43	Male	G4	Mutant	Methylated	80	G-CIMP	0.381778	Low	Training	Treated	Treated
TCGA-26-5132	0	286	Alive	74	Male	G4	WT	Methylated	60	Classical	0.617671	Low	Training	Treated	Treated
TCGA-26-5133	0	452	Alive	59	Male	G4	WT	Unmethylated	80	G-CIMP	0.172829	Low	Training	Treated	Treated
TCGA-26-5134	0	167	Alive	74	Male	G4	WT	Unmethylated	60	Proneural	2.073398	High	Testing	Untreated	Treated
TCGA-26-5135	1	270	Dead	72	Female	G4	WT	Methylated	NA	Proneural	1.246408	High	Training	NA	NA
TCGA-26-5136	1	577	Dead	78	Female	G4	WT	Methylated	NA	Mesenchymal	1.715617	High	Training	NA	NA
TCGA-26-5139	0	48	Alive	65	Female	G4	WT	Unmethylated	60	Mesenchymal	1.22691	High	Testing	Untreated	Untreated
TCGA-27-1830	1	154	Dead	57	Male	G4	WT	Unmethylated	80	Proneural	2.16978	High	Testing	Treated	Treated
TCGA-27-1831	1	505	Dead	66	Male	G4	WT	Unmethylated	80	Neural	1.09536	High	Training	Treated	Treated
TCGA-27-1832	1	300	Dead	59	Female	G4	WT	Unmethylated	100	Mesenchymal	1.670218	High	Training	Treated	Treated
TCGA-27-1834	1	1233	Dead	56	Male	G4	WT	Methylated	80	Neural	1.024834	Low	Training	Treated	Treated
TCGA-27-1835	1	648	Dead	53	Female	G4	WT	Methylated	80	Classical	0.853712	Low	Training	Treated	Treated
TCGA-27-1837	1	427	Dead	36	Male	G4	WT	Methylated	80	Classical	1.899875	High	Testing	Treated	Treated
TCGA-27-2519	1	550	Dead	48	Male	G4	WT	Unmethylated	80	Mesenchymal	2.957033	High	Training	Treated	Treated
TCGA-27-2521	1	510	Dead	34	Male	G4	Mutant	Methylated	80	G-CIMP	0.234014	Low	Testing	Treated	Treated
TCGA-27-2523	1	489	Dead	63	Male	G4	WT	Methylated	80	Classical	1.379457	High	Testing	Treated	Treated
TCGA-27-2524	1	231	Dead	56	Male	G4	WT	Unmethylated	80	Mesenchymal	0.494506	Low	Testing	Treated	Treated
TCGA-27-2526	1	87	Dead	79	Female	G4	WT	Unmethylated	40	Neural	0.764934	Low	Testing	Treated	Untreated
TCGA-27-2528	1	480	Dead	62	Male	G4	WT	Methylated	80	Classical	0.504031	Low	Testing	Treated	Treated
TCGA-28-1747	1	77	Dead	44	Male	G4	WT	Methylated	NA	Classical	1.26848	High	Testing	Treated	Treated
TCGA-28-1753	0	37	Alive	53	Male	G4	WT	Unmethylated	NA	Mesenchymal	1.321976	High	Testing	Untreated	Treated
TCGA-28-2509	0	145	Alive	77	Female	G4	WT	Methylated	80	Mesenchymal	0.62206	Low	Testing	Treated	Treated
TCGA-28-2513	0	222	Alive	69	Female	G4	WT	Unmethylated	80	Mesenchymal	1.92776	High	Training	Treated	Treated
TCGA-28-2514	0	160	Alive	45	Male	G4	WT	Unmethylated	60	Classical	0.965132	Low	Testing	Treated	Treated
TCGA-28-5204	1	454	Dead	72	Male	G4	WT	Unmethylated	80	Neural	1.43423	High	Training	Treated	Treated
TCGA-28-5207	1	343	Dead	71	Male	G4	WT	Unmethylated	70	Mesenchymal	0.694985	Low	Training	Treated	Treated
TCGA-28-5208	1	544	Dead	52	Male	G4	WT	Methylated	70	Mesenchymal	0.692142	Low	Training	Treated	Treated
TCGA-28-5209	0	442	Alive	66	Female	G4	WT	Methylated	NA	Mesenchymal	0.991533	Low	Training	Treated	Treated
TCGA-28-5215	1	335	Dead	62	Female	G4	WT	Methylated	90	Mesenchymal	1.282325	High	Training	Treated	Treated
TCGA-28-5216	0	415	Alive	52	Male	G4	WT	Unmethylated	80	Mesenchymal	0.722184	Low	Training	Treated	Treated
TCGA-28-5218	1	157	Dead	63	Male	G4	WT	Unmethylated	NA	Mesenchymal	2.771369	High	Training	Treated	Treated
TCGA-28-5220	1	388	Dead	67	Male	G4	WT	Unmethylated	90	Classical	0.849586	Low	Testing	Treated	Treated
TCGA-32-1970	1	468	Dead	59	Male	G4	WT	Unmethylated	NA	Classical	1.171662	Low	Training	Treated	Treated
TCGA-32-1980	1	36	Dead	72	Male	G4	WT	Unmethylated	NA	Neural	1.090867	Low	Testing	Untreated	Untreated
TCGA-32-1982	1	142	Dead	76	Female	G4	WT	Methylated	80	Neural	1.070619	Low	Testing	NA	NA
TCGA-32-2615	1	485	Dead	62	Male	G4	WT	Unmethylated	80	Mesenchymal	1.534527	High	Training	Treated	Treated
TCGA-32-2616	1	224	Dead	48	Female	G4	NA	Methylated	NA	Mesenchymal	3.066059	High	Training	Treated	Treated
TCGA-32-2632	1	269	Dead	80	Male	G4	WT	Unmethylated	NA	Mesenchymal	0.618968	Low	Training	NA	NA
TCGA-32-2634	0	693	Alive	82	Male	G4	WT	Methylated	NA	Proneural	0.794593	Low	Testing	Treated	Treated
TCGA-32-2638	1	766	Dead	67	Male	G4	WT	Methylated	NA	Classical	0.912361	Low	Testing	Treated	Treated
TCGA-32-4213	0	604	Alive	47	Female	G4	WT	Methylated	NA	Mesenchymal	1.083649	Low	Testing	Treated	Treated
TCGA-32-5222	1	585	Dead	66	Male	G4	WT	Methylated	NA	Proneural	0.390526	Low	Training	Treated	Treated
TCGA-41-2571	1	26	Dead	89	Male	G4	WT	Unmethylated	60	Proneural	1.338354	High	Testing	Treated	Untreated
TCGA-41-2572	1	406	Dead	67	Male	G4	WT	Unmethylated	NA	Classical	0.649637	Low	Testing	Treated	Treated
TCGA-41-3915	1	360	Dead	48	Male	G4	WT	Methylated	NA	Mesenchymal	0.995506	Low	Testing	Treated	Treated
TCGA-41-4097	1	6	Dead	63	Female	G4	WT	Unmethylated	NA	Mesenchymal	1.602511	High	Training	Untreated	Untreated
TCGA-41-5651	1	460	Dead	59	Female	G4	WT	Methylated	NA	Proneural	0.904324	Low	Training	Treated	Treated
TCGA-76-4925	1	146	Dead	76	Male	G4	WT	Methylated	100	Proneural	2.303884	High	Testing	Treated	Treated
TCGA-76-4926	1	138	Dead	68	Male	G4	WT	Unmethylated	80	Classical	1.401941	High	Training	Treated	Treated
TCGA-76-4927	1	535	Dead	58	Male	G4	WT	Unmethylated	80	Neural	2.548667	High	Testing	NA	NA
TCGA-76-4928	1	94	Dead	85	Female	G4	WT	Methylated	80	Classical	2.979728	High	Training	Treated	Treated
TCGA-76-4929	1	111	Dead	76	Female	G4	WT	Methylated	80	Neural	1.769521	High	Training	NA	NA
TCGA-76-4931	1	279	Dead	70	Female	G4	WT	Unmethylated	80	Classical	1.213032	High	Training	Treated	Treated
TCGA-76-4932	1	1458	Dead	50	Female	G4	WT	Methylated	80	Proneural	0.669549	Low	Training	Treated	Treated

GBM, glioblastoma multiforme; G-CIMP, glioma CpG island methylator phenotype; NA, not available; TCGA, The Cancer Genome Atlas; WT, wild type; IDH, isocitrate dehydrogenase.

https://dx.doi.org/10.21037/tcr-22-1592

Table S2 The clinical information of CGGA cohorts

CGGA_ID	futime	fustat	Grade	Gender	Age, year	Radio_status	Chemo_status	IDH_mutation_status	1p19q_codeletion_status	MGMTp_methylation_status	riskScore	Risk
CGGA_139	694	1	WHO IV	Male	59	1	1	Mutant	Non-codel	Un-methylated	13700.63	High
CGGA_1017	768	1	WHO IV	Female	29	1	0	Wild type	Non-codel	Un-methylated	11912.59	High
CGGA_1420	364	1	WHO IV	Male	60	1	1	Wild type	Non-codel	Methylated	4484.713	High
CGGA_1571	412	0	WHO IV	Female	43	1	1	Mutant	Non-codel	Methylated	4224.402	High
CGGA_P112	834	1	WHO IV	Male	65	1	1	Wild type	Non-codel	NA	2151.044	High
CGGA_1769	1854	0	WHO IV	Female	49	0	1	Wild type	Non-codel	Methylated	1029.878	High
CGGA_1750	250	1	WHO IV	Female	52	1	1	Wild type	Non-codel	Methylated	418.5919	High
CGGA_1501	222	1	WHO IV	Male	58	1	1	NA	Non-codel	Methylated	132.9349	High
CGGA_1452	468	1	WHO IV	Male	53	1	1	Wild type	Non-codel	Methylated	72.22825	High
CGGA_1840	1179	0	WHO IV	Female	58	1	1	Wild type	Non-codel	Methylated	69.06815	High
CGGA_1534	27	1	WHO IV	Female	58	0	0	Mutant	Non-codel	Un-methylated	63.15978	High
CGGA_1500	108	1	WHO IV	Female	45	1	1	Wild type	Non-codel	Un-methylated	57.82887	High
CGGA_1740	363	1	WHO IV	Female	50	0	0	Wild type	Non-codel	Methylated	47.16943	High
CGGA_1735	813	1	WHO IV	Male	54	1	1	Wild type	Non-codel	Un-methylated	41.02415	High
CGGA_P15	723	1	WHO IV	Male	49	1	1	NA	Non-codel	NA	38.15733	High
CGGA_1870	1556	0	WHO IV	Male	62	1	1	Mutant	Codel	Un-methylated	28.15274	High
CGGA_P22	406	1	WHO IV	Male	62	1	1	Wild type	Non-codel	NA	20.47522	High
CGGA_1041	3593	0	WHO IV	Male	58	1	1	Wild type	Non-codel	Un-methylated	20.21255	High
CGGA_1539	2462	0	WHO IV	Male	61	1	1	Mutant	Non-codel	Methylated	16.24608	High
CGGA_1690	592	1	WHO IV	Male	60	1	1	Wild type	Non-codel	Un-methylated	13.95259	High
CGGA_1472	1025	1	WHO IV	Male	34	0	0	NA	Non-codel	Methylated	13.74482	High
CGGA_1548	1054	1	WHO IV	Male	53	1	1	Wild type	Non-codel	Un-methylated	12.62223	High
CGGA_1326	322	1	WHO IV	Male	45	1	0	Mutant	Non-codel	Un-methylated	10.999	High
CGGA_1380	291	1	WHO IV	Male	46	1	1	Wild type	Non-codel	Methylated	9.251914	High
CGGA_P100	268	1	WHO IV	Male	67	NA	NA	Wild type	Non-codel	NA	8.716854	High
CGGA_1476	299	1	WHO IV	Female	53	0	0	Wild type	Non-codel	Methylated	8.392699	High
CGGA_1698	388	1	WHO IV	Female	55	0	0	Wild type	Non-codel	Methylated	8.193378	High
CGGA_1371	2791	0	WHO IV	Male	68	1	1	Wild type	Non-codel	Methylated	7.660351	High
CGGA_1727	1980	0	WHO IV	Male	48	1	1	Mutant	Non-codel	Un-methylated	7.116809	High
CGGA_1749	401	1	WHO IV	Female	44	1	1	Wild type	Non-codel	Un-methylated	7.100204	High
CGGA_1713	332	1	WHO IV	Male	62	1	1	Wild type	Non-codel	Methylated	7.097641	High
CGGA_1529	583	1	WHO IV	Male	63	NA	NA	Wild type	Non-codel	Un-methylated	6.668938	High
CGGA_1826	44	1	WHO IV	Female	70	0	0	Wild type	Non-codel	Methylated	5.82109	High
CGGA_1444	378	1	WHO IV	Female	68	1	1	Wild type	Non-codel	Methylated	5.733422	High
CGGA_1382	284	1	WHO IV	Male	57	1	1	Wild type	Non-codel	Methylated	5.623735	High
CGGA_1236	191	1	WHO IV	Female	47	0	0	Wild type	Non-codel	Methylated	5.590901	High
CGGA_1521	205	1	WHO IV	Female	63	1	1	Wild type	Non-codel	Methylated	5.174618	High
CGGA_509	623	1	WHO IV	Male	38	1	0	Wild type	Non-codel	Un-methylated	4.994979	High
CGGA_1559	603	1	WHO IV	Male	63	0	1	Mutant	Codel	Methylated	4.888849	High
CGGA_1728	917	1	WHO IV	Male	45	1	1	Mutant	Non-codel	Un-methylated	4.797313	High
CGGA_1595	2363	0	WHO IV	Female	34	1	1	NA	Non-codel	Un-methylated	4.706975	High
CGGA_1103	585	1	WHO IV	Female	35	1	1	Mutant	Non-codel	Methylated	4.328651	High
CGGA_1172	3131	0	WHO IV	Female	36	1	1	Mutant	Non-codel	Methylated	4.297041	High
CGGA_1256	2557	0	WHO IV	Female	52	1	1	NA	Non-codel	Methylated	4.012705	High
CGGA_1135	1244	1	WHO IV	Male	40	1	1	Wild type	Non-codel	Un-methylated	3.93855	High
CGGA_1433	394	1	WHO IV	Female	72	1	1	Wild type	Non-codel	Un-methylated	3.805769	High
CGGA_1596	205	1	WHO IV	Male	63	1	1	Wild type	Non-codel	Methylated	3.545952	High
CGGA_1812	780	1	WHO IV	Male	65	NA	NA	Wild type	Non-codel	Un-methylated	3.488737	High
CGGA_1807	247	1	WHO IV	Female	65	NA	NA	Wild type	Non-codel	Methylated	3.417393	High
CGGA_1694	624	1	WHO IV	Male	55	1	1	Wild type	Non-codel	Un-methylated	3.370004	High
CGGA_831	546	1	WHO IV	Female	55	1	1	Wild type	Non-codel	Un-methylated	3.303636	High
CGGA_1564	190	1	WHO IV	Male	48	1	1	Wild type	Non-codel	Un-methylated	3.265481	High
CGGA_1392	473	1	WHO IV	Male	62	1	1	Wild type	Non-codel	Un-methylated	3.045552	High
CGGA_1138	411	1	WHO IV	Male	54	1	1	Wild type	Non-codel	Un-methylated	2.848698	High
CGGA_1626	696	1	WHO IV	Male	66	1	1	Wild type	Non-codel	Un-methylated	2.770323	High
CGGA_1744	1936	0	WHO IV	Male	51	1	1	NA	Non-codel	Methylated	2.629381	High
CGGA_1546	223	1	WHO IV	Male	56	0	1	Wild type	Non-codel	Un-methylated	2.525209	High
CGGA_1551	347	1	WHO IV	Female	50	1	1	NA	Non-codel	Un-methylated	2.402468	High
CGGA_1543	723	1	WHO IV	Male	57	1	0	Mutant	Non-codel	Un-methylated	2.376964	High
CGGA_1612	718	1	WHO IV	Male	68	1	1	Wild type	Non-codel	Un-methylated	2.305388	High
CGGA_1075	398	1	WHO IV	Male	72	1	1	Wild type	Non-codel	Un-methylated	2.159129	High
CGGA_1601	710	1	WHO IV	Male	66	1	1	Wild type	Non-codel	Methylated	2.100128	High
CGGA_1391	426	0	WHO IV	Male	62	1	1	Wild type	Non-codel	Un-methylated	2.08978	High
CGGA_1764	710	1	WHO IV	Male	33	1	1	Mutant	Non-codel	Un-methylated	2.067779	High
CGGA_1833	494	1	WHO IV	Female	60	1	1	Wild type	Non-codel	Methylated	1.932302	High
CGGA_1901	540	1	WHO IV	Male	60	1	1	Wild type	Non-codel	Methylated	1.841542	High
CGGA_1817	399	1	WHO IV	Female	72	1	1	Wild type	Non-codel	Methylated	1.841531	Low
CGGA_1036	806	1	WHO IV	Male	41	1	1	Wild type	Non-codel	Methylated	1.840055	Low
CGGA_1537	97	1	WHO IV	Male	73	0	0	Wild type	Non-codel	Methylated	1.832147	Low
CGGA_1451	438	1	WHO IV	Female	45	1	1	Wild type	Non-codel	Un-methylated	1.768326	Low
CGGA_1134	59	1	WHO IV	Female	56	0	1	Wild type	Non-codel	Methylated	1.720361	Low
CGGA_1650	1283	1	WHO IV	Male	36	1	1	Mutant	Non-codel	Methylated	1.696587	Low
CGGA_1708	1122	1	WHO IV	Female	54	1	1	Wild type	Non-codel	Methylated	1.693432	Low
CGGA_1586	232	1	WHO IV	Female	55	1	1	Wild type	Non-codel	Un-methylated	1.619538	Low
CGGA_1354	530	1	WHO IV	Female	40	1	1	Wild type	Non-codel	Methylated	1.56303	Low
CGGA_1410	825	1	WHO IV	Female	27	1	1	Wild type	Non-codel	Methylated	1.554541	Low
CGGA_P609	726	0	WHO IV	Female	19	1	1	Wild type	Non-codel	Un-methylated	1.509591	Low
CGGA_1478	542	1	WHO IV	Female	72	1	1	Wild type	Non-codel	Methylated	1.490135	Low
CGGA_1441	1882	1	WHO IV	Male	70	1	1	Wild type	Non-codel	Methylated	1.488041	Low
CGGA_1758	414	1	WHO IV	Female	45	1	1	Wild type	Non-codel	Methylated	1.444681	Low
CGGA_P102	1269	1	WHO IV	Male	30	1	1	Mutant	Non-codel	NA	1.422524	Low
CGGA_1613	250	0	WHO IV	Male	53	1	1	Wild type	Non-codel	Methylated	1.401937	Low
CGGA_1699	2088	0	WHO IV	Female	41	0	1	Mutant	NA	Un-methylated	1.388717	Low
CGGA_1457	312	1	WHO IV	Male	60	1	1	Wild type	Non-codel	Methylated	1.306695	Low
CGGA_1644	173	1	WHO IV	Male	48	1	1	Wild type	Non-codel	Methylated	1.280691	Low
CGGA_1418	287	1	WHO IV	Female	73	1	1	Wild type	NA	Un-methylated	1.246618	Low
CGGA_1597	174	1	WHO IV	Male	58	1	0	Wild type	Non-codel	Methylated	1.234466	Low
CGGA_1106	420	1	WHO IV	Male	37	1	0	Wild type	Non-codel	Methylated	1.233681	Low
CGGA_P178	1442	0	WHO IV	Female	52	1	1	Wild type	NA	Methylated	1.228416	Low
CGGA_P28	107	1	WHO IV	Male	61	0	0	Wild type	Non-codel	NA	1.223842	Low
CGGA_1462	174	1	WHO IV	Male	49	1	1	Wild type	Non-codel	Methylated	1.204831	Low
CGGA_1542	184	0	WHO IV	Male	26	1	1	Mutant	NA	Un-methylated	1.18985	Low
CGGA_1426	133	1	WHO IV	Female	50	1	1	Wild type	Non-codel	Un-methylated	1.160183	Low
CGGA_1706	2068	0	WHO IV	Male	60	1	1	Wild type	Non-codel	NA	1.155537	Low
CGGA_1681	346	1	WHO IV	Female	58	1	1	Wild type	Codel	Methylated	1.143278	Low
CGGA_1142	1005	1	WHO IV	Male	60	1	1	Wild type	Non-codel	Un-methylated	1.089902	Low
CGGA_1678	657	1	WHO IV	Male	51	1	1	Wild type	NA	Methylated	1.056915	Low
CGGA_1402	2742	0	WHO IV	Male	30	1	1	Wild type	Non-codel	Methylated	1.03731	Low
CGGA_1736	938	1	WHO IV	Female	57	1	1	Wild type	Non-codel	Un-methylated	0.995717	Low
CGGA_1353	1022	1	WHO IV	Male	65	1	1	Wild type	Non-codel	Un-methylated	0.980293	Low
CGGA_1560	459	1	WHO IV	Female	35	1	1	Mutant	Non-codel	Methylated	0.967865	Low
CGGA_1365	253	1	WHO IV	Male	55	1	1	Wild type	NA	Methylated	0.950972	Low
CGGA_1866	127	1	WHO IV	Male	68	1	1	Wild type	Non-codel	Un-methylated	0.90668	Low
CGGA_1819	1005	1	WHO IV	Male	55	0	1	Wild type	Non-codel	Methylated	0.902441	Low
CGGA_P160	219	1	WHO IV	Female	72	1	1	Wild type	Non-codel	NA	0.898032	Low
CGGA_1467	866	1	WHO IV	Male	58	1	0	Mutant	NA	Un-methylated	0.865512	Low
CGGA_1767	86	1	WHO IV	Male	63	0	0	Wild type	NA	Methylated	0.863224	Low
CGGA_1687	2118	0	WHO IV	Male	14	1	1	Wild type	Non-codel	Un-methylated	0.859015	Low
CGGA_P143	261	1	WHO IV	Female	66	1	1	Wild type	Non-codel	NA	0.853727	Low
CGGA_1461	226	1	WHO IV	Female	60	1	1	Wild type	Non-codel	Un-methylated	0.832466	Low
CGGA_1666	249	1	WHO IV	Male	60	1	1	Wild type	NA	Methylated	0.816079	Low
CGGA_1282	1116	1	WHO IV	Female	33	1	1	Wild type	Non-codel	Un-methylated	0.813022	Low
CGGA_1086	1977	1	WHO IV	Female	65	1	1	Wild type	NA	Methylated	0.810788	Low
CGGA_1635	332	1	WHO IV	Female	43	1	1	Wild type	NA	Un-methylated	0.802611	Low
CGGA_1491	246	1	WHO IV	Male	29	1	1	Mutant	Non-codel	Un-methylated	0.786287	Low
CGGA_1709	415	1	WHO IV	Male	47	1	1	Wild type	Non-codel	Un-methylated	0.770231	Low
CGGA_1503	777	1	WHO IV	Male	47	1	1	Wild type	NA	Un-methylated	0.76868	Low
CGGA_1425	640	1	WHO IV	Female	22	1	1	Wild type	Codel	Methylated	0.713432	Low
CGGA_P116	305	1	WHO IV	Male	58	1	NA	Wild type	NA	NA	0.70161	Low
CGGA_1403	679	1	WHO IV	Female	43	1	1	Wild type	Non-codel	Methylated	0.701189	Low
CGGA_P136	842	1	WHO IV	Female	41	1	1	Wild type	NA	NA	0.695196	Low
CGGA_1780	1826	0	WHO IV	Female	57	0	1	Wild type	NA	NA	0.684277	Low
CGGA_1634	366	1	WHO IV	Female	26	0	0	Wild type	Non-codel	Methylated	0.681855	Low
CGGA_1422	204	1	WHO IV	Male	76	1	1	Wild type	NA	Un-methylated	0.680168	Low
CGGA_1494	269	1	WHO IV	Male	21	1	1	Wild type	NA	Methylated	0.678442	Low
CGGA_P205	583	1	WHO IV	Male	66	1	1	Wild type	NA	NA	0.639481	Low
CGGA_P180	260	1	WHO IV	Male	47	1	1	Mutant	NA	NA	0.63623	Low
CGGA_1481	131	1	WHO IV	Male	55	0	0	Wild type	NA	Methylated	0.63525	Low
CGGA_1486	184	1	WHO IV	Male	45	1	1	Wild type	NA	Methylated	0.631435	Low
CGGA_1378	378	1	WHO IV	Male	47	1	1	Wild type	NA	Un-methylated	0.61457	Low
CGGA_1722	349	1	WHO IV	Female	60	1	1	Wild type	NA	Un-methylated	0.610515	Low
CGGA_P25	147	1	WHO IV	Male	64	1	1	Wild type	NA	NA	0.599144	Low
CGGA_P164	1553	0	WHO IV	Male	27	1	1	Wild type	NA	NA	0.594725	Low

CGGA, Chinese Glioma Genome Atlas; Codel, codeletion; NA, not available; WHO, World Health Organization; IDH, isocitrate dehydrogenase.

https://dx.doi.org/10.21037/tcr-22-1592